UNIVERSIDAD DE INVESTIGACIÓN DE TECNOLOGÍA EXPERIMENTAL YACHAY

Escuela de Ciencias Biológicas e Ingeniería

TÍTULO: Molecular Surface Interaction Modeling of Poly(vinyl pyrrolidone) on Multi-walled Carbon Nanotubes

Trabajo de integración curricular presentado como requisito para la obtención del título de Ingeniera Biomédica

Autor:
Veintimilla Carrion Keiko Sahori

Tutor:
Ph.D. Chacón Julio

Co-tutor:
Ph.D. Poblete Horacio

Urcuquí, enero 2023

AUTORÍA

Yo, **VEINTIMILLA CARRIO KEIKO SAHORI**, con cédula de identidad 1004441695, declaro que las ideas, juicios, valoraciones, interpretaciones, consultas bibliográficas, definiciones y conceptualizaciones expuestas en el presente trabajo; así cómo, los procedimientos y herramientas utilizadas en la investigación, son de absoluta responsabilidad de la autora del trabajo de integración curricular. Así mismo, me acojo a los reglamentos internos de la Universidad de Investigación de Tecnología Experimental Yachay.

Urcuquí, enero 2023.

Keiko Sahori Veintimilla Carrion
CI: 1004441695

AUTORIZACIÓN DE PUBLICACIÓN

Yo, **VEINTIMILLA CARRION KEIKO SAHORI,** con cédula de identidad 1004441695, cedo a la Universidad de Investigación de Tecnología Experimental Yachay, los derechos de publicación de la presente obra, sin que deba haber un reconocimiento económico por este concepto. Declaro además que el texto del presente trabajo de titulación no podrá ser cedido a ninguna empresa editorial para su publicación u otros fines, sin contar previamente con la autorización escrita de la Universidad.

Asimismo, autorizo a la Universidad que realice la digitalización y publicación de este trabajo de integración curricular en el repositorio virtual, de conformidad a lo dispuesto en el Art. 144 de la Ley Orgánica de Educación Superior

Urcuquí, enero 2023.

Keiko Sahori Veintimilla Carrion
CI: 1004441695

Acknowledgements

I thank my parents for their love, care and dedication during the years of my life, which has allowed me to reach and accomplish this first goal in my professional training. I also thank Dr. Julio Chacón for his academic support and for believing in me for the completion of this thesis. To Dr. Horacio Poblete for his important academic support, his unconditional patience in every doubt that arose, his concern and trust. To my friends, Mica, Paola, Jhuliana and Andrés, who made my time at the university a pleasant and important moment in my life. I would also like to thank the Bio-nanomaterials research group led by Dr. Horacio Poblete for his closeness and help at different times, especially Matias Zuñiga for his friendship and his willingness to share his knowledge with me. And to all those people who were with me in some way or another, either with a greeting or sharing in the day to day.

Resumen

En los últimos años se ha destacado el potencial de los nanotubos de carbono multipared (MWCNT) para su uso en aplicaciones biomédicas debido a sus propiedades químicas y físicas únicas. Sin embargo, el desarrollo de nuevos dispositivos con MWCNT se enfrenta a importantes retos, como la biocompatibilidad, la capacidad de dispersión y la disolución en disolventes polares de los CNTS. Entre las estrategias más utilizadas se encuentra el recubrimiento del nanotubo de carbono con moléculas capaces de interactuar con él y proporcionarle propiedades que lo hagan apto para un entorno biológico. La polivinilpirrolidona (PVP) es un polímero biocompatible que muestra una afinidad compleja por fármacos hidrofílicos e hidrofóbicos, lo que lo convierte en un candidato ideal para el recubrimiento de MWCNTs. Así, en el presente proyecto de tesis se realizó un estudio de la interacción del PVP con superficies de nanotubos de carbono para determinar el comportamiento del PVP con la superficie a través de herramientas computacionales. Se desarrollaron dos modelos de nanotubos de carbono para comprender la influencia de la estructura tubular y las múltiples capas en la interacción con los polímeros de PVP. El estudio identificó con el modelo SWCNT un fenómeno de envoltura y una distancia más cercana al PVP que el modelo de capas. El artículo concluye que la cantidad de polímero PVP utilizada con el CNT debe estimarse en función de la aplicación prevista, ya que las propiedades del nanotubo y del polímero pueden verse afectadas en función de su cantidad. Este estudio pone de relieve el uso potencial del PVP como material de recubrimiento de los MWCNT y proporciona información sobre la interacción entre el PVP y las superficies de los CNT, lo que podría contribuir al desarrollo de dispositivos biomédicos más seguros y eficaces.

Palabras clave: Nanotubos de Carbono Multipared (MWCNT), PVP, Interacción Superficial, Simulaciones Dinámicas

Abstract

In recent years, the potential of multi-walled carbon nanotubes (MWCNT) for use in biomedical applications has been highlighted due to their unique chemical and physical properties. However, the development of new MWCNT devices faces significant challenges, such as biocompatibility, dispersion capability, and dissolution in polar solvents. One of the most commonly used strategies is coating the carbon nanotubes with molecules capable of interacting with them and providing properties suitable for a biological environment. Polyvinylpyrrolidone (PVP) is a biocompatible polymer that exhibits complex affinity for hydrophilic and hydrophobic drugs, making it an ideal candidate for coating MWCNTs.

Therefore, in this thesis project, a study of the interaction between PVP and carbon nanotube surfaces was carried out to determine PVP behavior on the surface through computational tools. Two models of carbon nanotubes were developed to understand the influence of the tubular structure and multiple layers on interaction with PVP polymers. The study identified a wrapping phenomenon and a closer distance to PVP with the SWCNT model than the layer model. The article concludes that the amount of PVP polymer used with CNT should be estimated based on the intended application, as the properties of the nanotube and polymer may be affected depending on the amount. This study highlights the potential use of PVP as a coating material for MWCNTs and provides information on the interaction between PVP and CNT surfaces, which could contribute to the development of safer and more effective biomedical devices.

Keywords: Multi Wall Carbon Nanotube (MWCNT), PVP, Surface Interaction, Dynamics Simulations

Contents

List of Figures

List of Tables

Chapter 1

Introduction

Since their discovery, carbon nanotubes (CNTs) have been the subject of numerous studies focused on their exceptional properties such as high strength, toughness, flexibility, high surface area, high thermal conductivity, good electric conductivity, and chemical stability[1]. This opens up the possibility of a wide range of applications in many industries. For example, carbon nanotubes' rigidity and flexibility can be used to reinforce composite materials such as plastics and metal alloys[2]. In particular, the biomedical area is one of the most exciting and has a high volume of research related to the use of CNTs, as shown by the more than 23231 publications between 2012 and 2022 related to biomedical applications of CNTs found through the bibliographic search Scopus website.

For the study of CNT, different experimental methods and computational studies have been used which allow a deeper understanding of the system and materials under study. Thus, the collaboration between experimental and theoretical studies is vital for developing modern science and technology. In detail, there are a wide variety of computational tools for the description of physical and thermodynamic characteristics that can be studied at different scales. The theoretical studies allow the prediction of materials properties not yet experimentally synthesized and explain experimentally observed phenomena[3].In this context, the following thesis project aims to describe the multi-walled carbon nanotube surface and Poly(vinyl pyrrolidone) (PVP) polymer interaction through molecular dynamics simulation.

1.1 Carbon Nanotubes

Carbon is a highly versatile element resulting in the existence of a large number of carbon allotropes determined by the possibility of carbon atoms binding each other in different ways[4]. The molecular structure of these carbon allotropes depends on the hybridization of 2s and 2p orbitals (figure 1.1). Carbon can hybridize in sp, sp^2, or sp^3 forms. In sp^2 hybridized forms, graphene is generally the basic structure for other sp^2 carbons such as fullerenes and carbon nanotubes. In graphene, carbon atoms are densely organized in a regular sp^2 bonded atomic-scale honeycomb (hexagonal) pattern[5]. Carbon nanotubes can be defined as a sheet of graphene rolled into a cylinder, and some physical properties of CNTs are derived from graphene. However, the curvature produced for the tubular form of CNTs makes the sp^2 bonding protrude into the third dimension, achieving some of the characteristics of the sp^3 bonded materials. Therefore, CNT can exhibit mechanical and electrical properties between graphite and diamond[6].

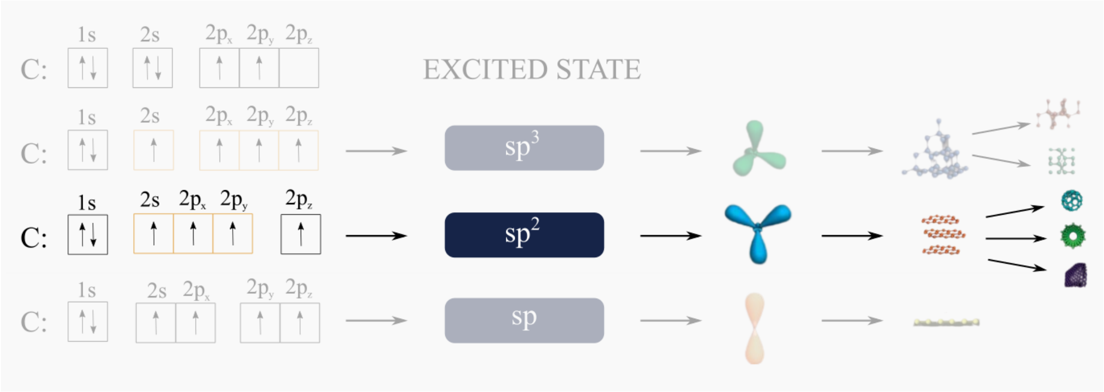

Figure 1.1: Schematic illustration of the three kinds of hybridization of carbon. The three different carbon hybridization states depend on how many p orbitals are implicated. In the case of sp hybridization, the form involves the $2s$ orbital with one of the $2p$ orbitals obtained from two sp orbitals in linear geometry with the angle of 180° between bonds. In the second hybridization, the $2s$ orbital pairs with two $2p$ orbitals, yielding three sp^2 orbitals.These are on the same plane, separated by an angle of 120°. In the third type of hybridization, $2s$ orbitals with three $2p$ orbitals form four sp^3 orbitals that have a tetrahedral shape with an angle of 109.5° between each bond.

1.1.1 Morphology and Atomic Structure of Carbon Nanotubes

CNT are typically grouped as single-walled carbon nanotubes (SWCNTs) (fig 1.2a) or multiwalled carbon nanotubes (MWCNTs) (fig 1.2b) according to the number of walls[6]. Iijima observed a single-wall carbon nanotube for the first time in 1993[7], while Iijima discovered MWCNTs in 1991[8], which consisted of multiple rolled layers of graphene. MWCNTs can have varied inner and outer diameters ranging from 0.4nm to a few nanometers in the inner diameter based on the number of layers. In contrast, they present sizes from 2nm to 30nm in the outer diameter in most cases[9].

The nanotube structure is determined by its chiral vector, corresponding to the cylinder's circumference when the graphene layer is rolled up into a tube. Depending on a pair of indices (n,m) and their possible values of theta angle (Θ) that describe the chiral vector (C), SWCNT can present three different forms: armchair, chiral, and zigzag. When $n = m$, $(\Theta) = 30°$, the nanotubes are named armchair; zigzag are the nanotubes with $m = 0$, $(\Theta) = 0°$, and named chiral when $m \neq 0$, $0 < (\Theta) < 30°$. The chiral vector $C= n(a1) + m(a2)$ (a1 and a2 are the base cell vectors of graphite) directly affects the electrical properties of CNTs; the armchair form is metallic, whereas other forms can make the nanotube a semiconductor. The chiral vector also determines the tube diameter d, and this vector defines the direction of rolling a graphene sheet[4,10] (fig 1.2c) . The structure of MWCNTs depends on how they are formed, and two structural models are used to classify them: the Parchment model and the Russian Doll model. The scroll

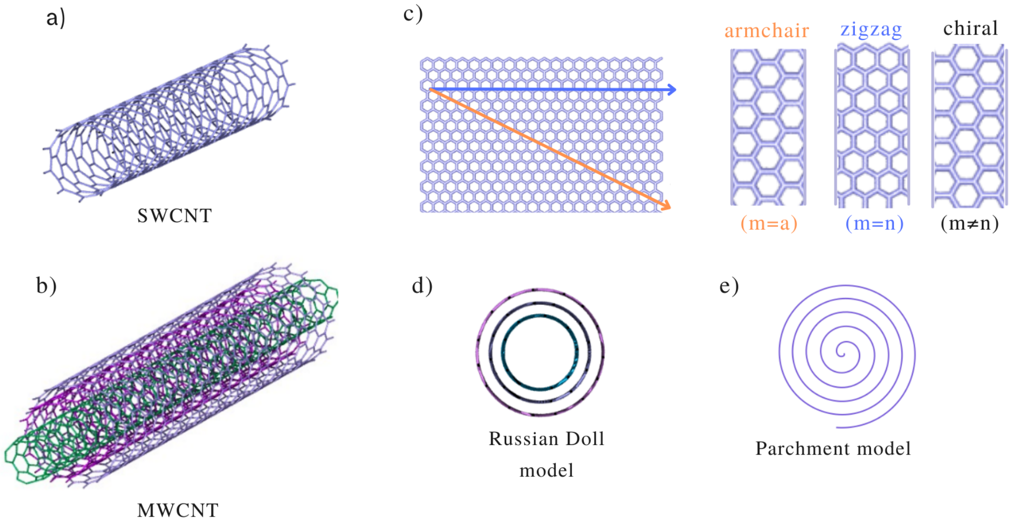

Figure 1.2: SWCNT and MWCNT structure types. a)Single Wall Carbon Nanotube model; b)Multi Wall Carbon Nanotube model, c)three types of SWNTs identified by the integers (n, m); d)russian model of MWCNT; e)parchment model of MWCNT

model involves a single SWCNT wound on itself several times (fig 1.2d). On the other hand, a CNT inside another CNT with larger diameters is a Russian doll model[9] (fig 1.2e) .

1.1.2 MWCNTs Properties

The nanotube application depends on its elastic response, the inelastic behavior and buckling, yield strength, and fracture-related experimental and theoretical investigation of these properties[8]. In general, CNTs have high axial strength and stiffness due to the sp^2 bond between carbon-carbon atoms. Some properties of MWCNTs differ from SWCNTs because of the number of layers they exhibit. The multilayer nature of MWCNTSs gives them a higher tensile strength than SWCNTs. However, the number of layers means a decrease in the elastic capacity of MWCNTs. Other significant differences include the greater ease of bulk synthesis, production without the need of catalysis, high purity, complex structures, and more significant accumulation in the body of MWCNTs[9,11]. Further details of the properties of MWCNTs are given in Table 1.

Table 1.1: Properties MWCNTs.

Type	Name	Description
Mechanical properties	Young's Modulus (GPa)	1200
	Tensile strenght (GPa)	2.5
	Density (g/cm^3)	2.6
Thermal properties		The graphene composition provides CNTs to remain stable at very high temperatures (400K). Also, their lower dimensional structure allows CNTs to maximize their configuration and vibration entropy at a bit of energy cost, giving rise to a thermal contraction in length and volume up to temperatures of several hundred degrees Celsius[12] .
Surface properties	Physical adsorptions	CNTs/molecule interaction capacity by non-covalent bonding through different adsorption forces, such as hydrogen bonds, Van der Waals forces, pi-pi interaction, and electrostatic forces. This interaction retains the structures integrity and network of CNTs[13]
	Chemical interaction	A covalent functionalization by covalent linkages of functional molecules to CNTs. There are two types depending of interaction site[14]: Sidewall functionalization: hybridation from sp^2 to sp^3 and loss of conjugation. Defect functionalization: transformations of defect sites that can be the open end and holes in sidewalls.

1.1.3 Biomedical application of MWCNTs

According to Saliev (2019), the principal and initial research interest in using CNTs are bio-sensing, accounting for the 700 research articles published until 2019[15]. Multi-wall carbon nanotubes have been specially tested for various biosensors due to their easy protein immobilization support. At the same time, maintain the inherent activity and as a sensing element to detect and monitor several diseases[16]. MWCNTs increase the surface area of electrodes and improve electron transfer, increasing the sensitivity of electrochemical biosensors[17] through enzyme[18] , antibodies-antigens, DNA[19] , and non-biomolecules-based[20] . However, the use of carbon nanotubes is not limited to biosensors.

They are also being widely studied in tissue engineering, the target of therapies and implants (see Figure 1.3).

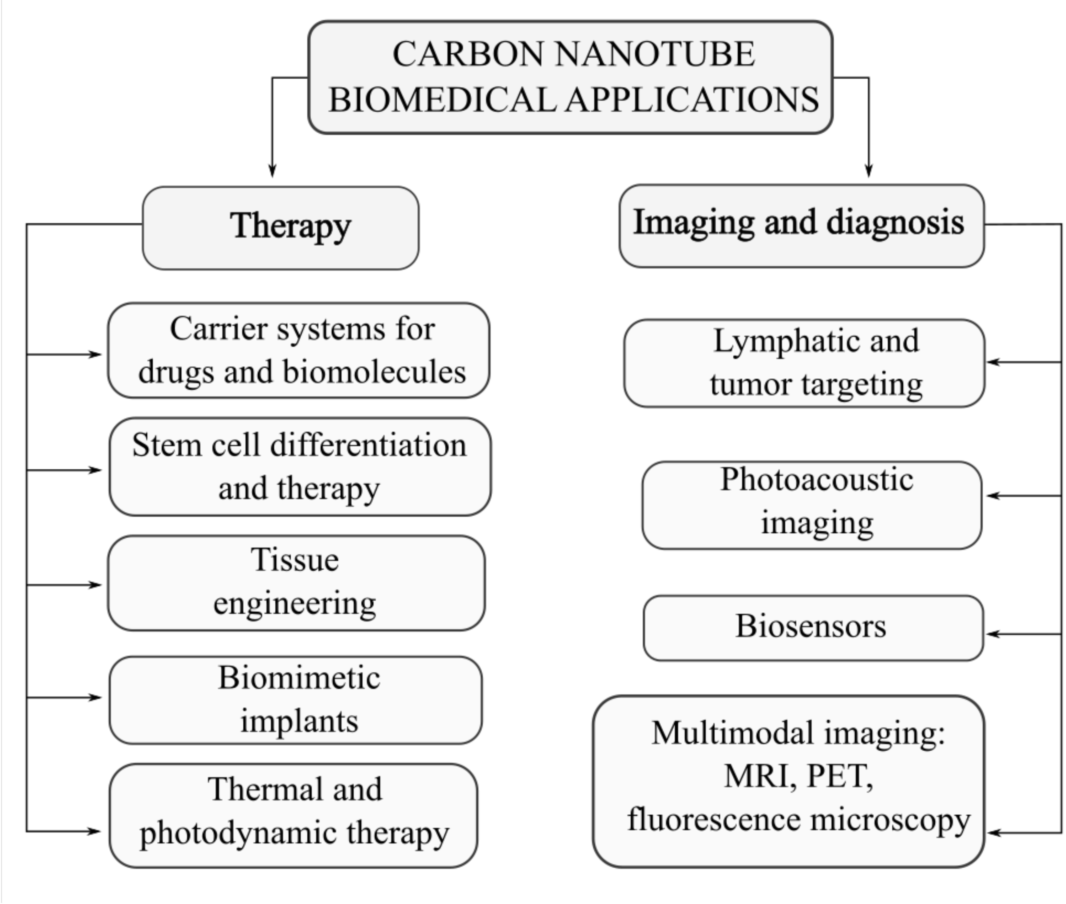

Figure 1.3: CNTs in major biomedical applications.

CNTs are an anti-cancer drug, genes, and proteins for chemotherapy. Carbon nanotubes offer an opportunity to shelter anti-cancer drugs, thus their ability to accumulate in the desired site and lower their toxicity for the organism[21,22]. In the tissue engineering, polymer-based scaffolds have been fabricated for neural[23] , cardiac[24] , and bone[25] tissue with a reinforcement filler of MWCNTs, improving mechanical and electrical properties. The addition of CNTs in the polymer matrix contributes to the conductivity of the nerve scaffold and enhances the nerve cell response. It also improves the elastic strength, conductivity, and biological response of cardiac scaffolds, and It is helpful to reinforce the mechanical properties and biological properties in bone tissue engineering[13].In addition, the chemical and physical properties of CNTs can contribute to the field of artificial implants. They can be employed as implants in artificial joints and other implants without host rejection and act as bone substitutes if filled with calcium and arranged in the bone structure[9]. Finally, an attractive use and characteristic of MWCNT is their antibacterial activity. This property can be activated in different ways onto the microbial surface. The impurities associated with the MWCNTs can be closely associated with the membrane surface or induce reactive oxygen species generation, ultimately leading to cell death and DNA damage. These antibacterial activities depend on various factors such as density, diameter,addition of functional groups on CNT surface , length, and purity of carbon nanotubes[24].

1.1.4 Biocompatibility and cytotoxicity of CNTs

The application of CNT in the biomedical field requires a few challenges to be overcome. The first one is related to impurities deposited on the surface of the CNTs in the synthesized process that involve metal catalysts such as iron, cobalt, and nickel that could induce oxidative stress and anti-depletion[26,27]This is a real challenge because it is very costly to prepare on a large scale for the purification process and the possible alteration of the CNT structure. The other main challenge is surface defect/imperfection resulting in pulmonary toxicity. At the same time, needle-like nanotubes can affect the pleura[28,29]Another challenge of CNTs is their aspect ratio, and their hydrophobic solid nature often results in agglomerations and lack of dispersion and solubility in water and most organic solvents[16,29] Figure 1.4.

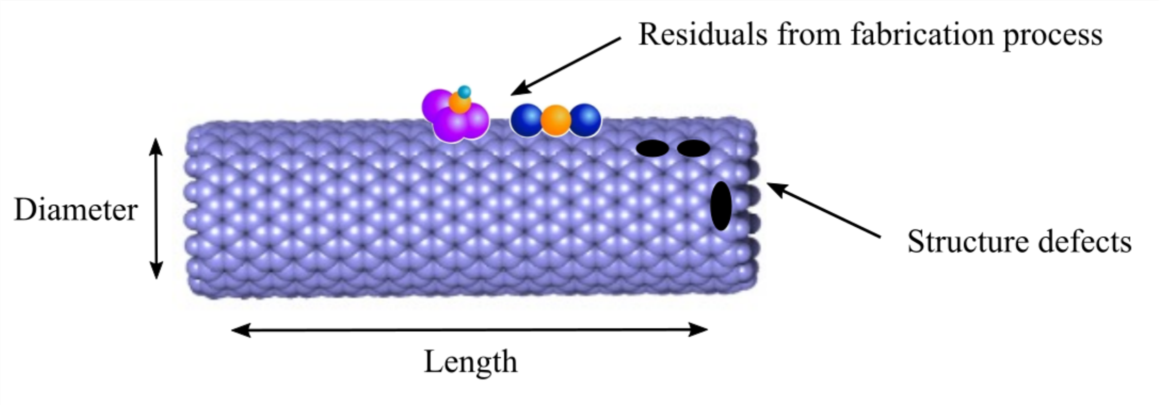

Figure 1.4: Schematic illustration of several factors that might cause CNTs toxicity.

1.1.5 Surface Modification of CNTs

Essentially, polymers can be utilized as a potential strategy to approach the unique properties of CNTs and enhance their solubility and compatibility with biological systems. Polymers are large molecules composed of necklaces of functional groups able to interact via covalent (chemical) or non-covalent interactions. This section details these strategies, emphasizing the especially suitable methods for biomedical applications (see Figure 1.5)[16,30] .

Covalent Functionalization of Carbon Nanotubes

The chemical interaction with CNTs is based on functional groups onto carbon forms of CNTs resulting in strong coupling between components. The chemical details of the exposed surface determine the range of resulting interactions. It can be performed at the end caps in the nanotube or at their sidewalls which have many defects modifying the tube hybridization fromsp^2 to sp^3 that change the conjugated-electron framework of CNTs. Also, defects on the nanotube sidewall are introduced, resulting in losing intrinsic properties such as NIR fluorescence and Raman scattering characteristics. However, the covalent functionalization is widely used for sensing and bio-imaging application and various strategies for their use in biomedical purposes, including surface oxidation of CNTs, cycloaddition reactions, radical additions, and their subsequent privatizations with biologically relevant molecules[31,32].

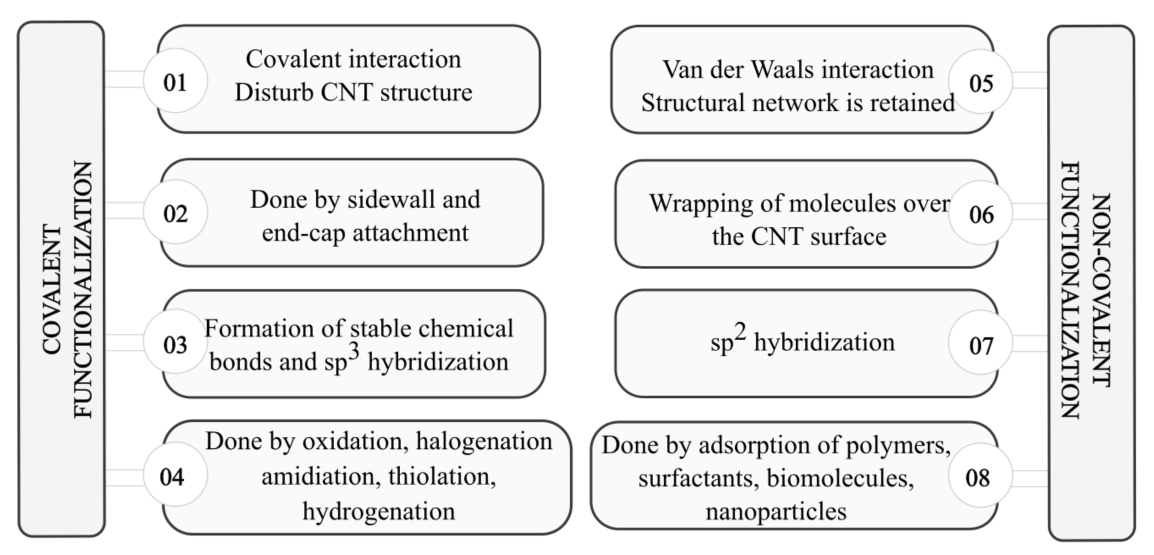

Figure 1.5: Comparison between covalent and non-covalent functionalization. Carbon nanotubes can be functionalized using two approaches: covalent or non-covalent.In the former scheme, various chemical approaches have been developed toward forming chemical bonds with carbon nanotubes, such as either at the end or on the sidewalls. Covalent functionalization is limited because it generates sp^3 hybridization on the carbon sites of CNTs, which blocks the transitions of p-electrons. Consequently, novel CNT properties may be lost. Non-covalent functionalization of CNTs has the potential to be used for supramolecular adsorption or wrapping of various functional groups, surfactants, polymers, or biomolecules. Non-covalent functionalization can enhance the solubility and dispersibility of CNTs without changing the sp^2 hybridization.

Non-covalent functionalization of carbon nanotubes

Alternatively, non-covalent functionalization allows high dispersable and processable CNTs without disturbing the carbon lattice via weak forces such as hydrophobic interactions, hydrogen bonds, - stacking, and Vdw forces. The molecular weight and density of molecular layers controlled the range and strength of the interaction, which means that they do not depend on the detailed chemistry of the CNT-molecular interface. Additionally, the range and depth of the combined systems' inter-molecular effective potential and behavior are composed of polymer structure, surface forces, geometry, and topology. In detail, the range of vdW force interactions through CNT is determined by the nanometric length scale characteristic of two of the three dimensions of the tube. A repulsive (steric) barrier whose range and strength can be controlled by the polymer chain length and surface density. The range of the attractive vdW interactions between particles is determined by the dimensions of the particle. In general the interaction range is a few times the particle size. Thus, in the case of CNT the range of the attractive interactions is a couple of nanometers and adsorption of relatively short polymers, in good solvent conditions, suffices to present a steric barrier at a distance larger than the attractive inter-tube minimum, preventing tube aggregation[30,33] . The absorbed or wrapped onto CNT through non-covalent interaction is available to many amphiphilic molecules such as RNA, DNA, peptides, proteins, polymers, etc. The concentration of these amphiphilic molecules on the surface, temperature, ultra sonications, and the chemical characteristic of the nanotube surface determine the dispersion of CNT. When nonionic surfactants are used, they dominate the steric stabilization by adsorbed nonionic surfactant or polymer layers. In contrast, the dispersal of CNTs through electrostatic repulsion between similarly charged groups is facilitated by ionic amphiphilic molecules[31]

The advantage of a non-covalent interaction is that it maintains the final structural properties of the material and does not destroy the conjugate system of the CNT's sidewalls. In addition, the high specific surface area of CNTs provides a high loading capacity for adhering molecules. Consequently, CNT presents their desired properties while improving their solubility quite remarkably, keeping the ability in various solutions and functional groups available for further bio-conjugation[31–33] .

1.2 Polyvinylpyrrolidone (PVP)

Polyvinylpyrrolidone (PVP), also called Povidone, is a polymer synthesized via a free radical polymerization reaction of the monomer N-vinylpyrrolidone patented by Reppe in 1938. The monomer comprises 1 oxygen, 1 nitrogen, 6 carbons, and 9 hydrogens, and the chain creates linkages at the extreme methane molecule (see Figure 1.6). The synthesis procedure involves a five-step reaction using acetylene as the starting material to obtain N-vinylpyrrolidone[34]. PVP is a water-soluble polymer, non-toxic, inert, bio-compatible, non-ionic, temperature resistant, and has a complex affinity for hydrophilic and hydrophobic drugs[35 36]. Initially, PVP was used as blood plasma substitute and as a hair fixative agent. Later, PVP gained a valuable role in the cosmetic, pharmaceutical, and food industries due to its exciting physical, chemical, and biological properties[37] given in Table 2.

Since PVP was proposed for the medical, pharmaceutical, and food industries, extensive research has developed its pharmacokinetics and toxicological profile. It was found that the absorption, distribution, metabolism, and

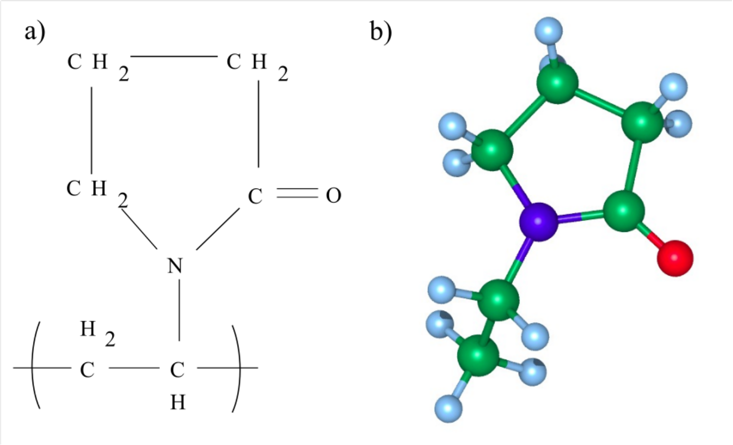

Figure 1.6: a)Structure of the repeating unit and b)three-dimensional structure of the PVP.

excretion (ADME) of PVP have a relationship with the molecular weight of the polymer, route administration, and dose frequency[38]. Ravin et al. reported that PVP shows a longer retention time 39 . Several studies conclude that there is no minimal absorption of PVP and evidence of the PVP's metabolism in the biological system, either in animals or humans[38]Regarding the toxicology of PVP, studies in animals like pigs, rats, dogs, and rabbits show no acute or sub-chronic, or chronic toxicity of PVP by oral administration. Karakul et al. mentioned that there is no evidence of toxicity in histopathology, clinical chemistry, and hematology except diarrhea in high doses[39]. Also, PVP is safe for its use through ocular, dermal and parental administration, the last in terms of low molecular weight[40]. Thus, it can be used in diverse forms and structures such as nanofibers, tablets, hydrogels, nanoparticles, and microneedles for different biomedical applications[41 42] .

Table 1.2: Properties of PVP.

Type	Name	Description
Physical properties	Physical description	Fine, odorless, hygroscopic, off white, amorphous
	Molecular formula	(C6H9NO) n
	Molecular weight	2500 to 2900000 Da depends on synthesize method used[43]
Chemical properties	Chemical structure	PVP is comprised of functional groups C-0, C–N, CH2 with a strong hydrophilic moiety (pyrrolidone) and a strong hydrophobic moiety (alkyl group)[34]
	Solubility	Soluble in water and organic solvents such as alcohols, amines, chloroform, methylene chloride,and nitroparaffins. Insoluble in ether, esters ketones, hydrocarbons and some chlorinated hydrocarbons[44]
	Compatibility	High compatibility in film and solution form, with natural and synthetic resins, most inorganic salts and many with many natural and synthetic resins[45]
Biological properties	Complex formation	PVP forms complexes with many substances resulting in either stabilization or precipitation. Also It provides stability to the tablet formulations and it may be combined with other reagents to obtain soft clear gelatin capsules of insoluble drugs[46].
	Protective-colloid action	The addition of small quantities of PVP efficiently stabilizes suspensions, emulsions, and dispersion.

1.3 Biomedical Application of MWCNTs/PVP

As mentioned above, MWCNTs stand out for their unique electromechanical properties. However, they cannot be used directly in the body and require to be used in a nanocomposite or functionalized. The PVP polymer attracts researchers for its interaction with MWCNTs due to its easy processability, unique transparency, biocompatible and non-toxic features. PVP is safe to be utilized in the health industry, especially in medicine and food. MWCNTs and PVP are advantageous for biomedical applications such as drug delivery, nanoparticle support, coatings, and cell growth surfaces. The amphiphilic nature of PVP allows it to disperse CNTs in water. Therefore, CNTs are mixed with PVP to be used as supports for nanoparticles avoiding agglomeration problems and improving the stability of nanoparticles (Np). In this way, CNTs can provide the expected electromechanical properties as expressed by Juixiao

Sun et al., which successfully developed a Pt electrocatalyst supported on MWCNT and further coated with ABPBI layer that could be used for accurate DMFC long-term operation without any deterioration in fuel cell performance[47].

Similarly, Haghighat and Mokhtary developed a magnetic decorate carboxylic acid functionalized multi-walled carbon nanotube (MWCNT-Fe_3O_4) that obtain better distribution of CNTs in a PVP matrix. Also, the addition of MWCNT-Fe_3O_4 ($5w/w$) to PVP improved the thermal properties of pure polyvinylpyrrolidone. Carbon nanotube (CNT) polymer composites have critical potential applications in functionalizing therapeutic biomolecules. Hence, the prepared polymer nanocomposite will play a significant role in water treatment and biomedical applications[48]. On the other hand, Bulbul et al. incorporated the MWCNTs, a fibrous structure initially composed of PVP/PVP for controlled drug delivery. The mechanical properties decrease significantly with drug release from the electrospun fiber. In this context, the incorporation of MWCNTs significantly increases the affected properties.

Moreover, it increases the encapsulation efficiency of the studied drug called "TCH". CNTs are chosen over other inorganic NPs because of their high aspect ratios, nano-sized sturdy tubes, and high surface areas[49]. While Maziukiewicz et al. incorporated MWCNTs, a mixture of two polymers of different hydrophobic characters: poly(maleic-alt-1-octadecene) and polyvinylpyrrolidone, to produce composite coatings with varied hydrophobicity. They research the composite coating stability, surface roughness, thickness, and wettability to establish the influence of the MWCNTs content on the overall physicochemical properties and MWCNT-polymer interaction. They were able to determine the presence of covalent molecular interaction between polymers and MWCNT. These coatings proved viable for cell adhesion and mimic stability, providing good support for cell growth and propagation[50].

1.4 Computational Methodologies

Nowadays, modeling and simulating techniques are a robust complement of experimental methods for the nanostructure-based materials development. Experimental techniques are usually used to design and explore the potential of these nanostructures; however, simulation methods mean a guide of experimentation and allow a faster description of the behavior of the bio-nanosystem. These techniques allow researchers to perform a series of simulations changing variable values to identify the laboratory experiments that are most likely to solve the problem under study. That means reducing the cost and a time acceleration of various steps in developing biomaterials. Researchers can perform a series of computational models to examine the health risk of nanomaterials prior to their synthesis and biological testing. In addition, the computational algorithms can give an acceptable description of physicochemical and structural properties such as shape, size, chemical reactivity, and toxicity. Similarly, computational modeling allows researchers to carry out studies at the atomistic level of great scientific relevance because the effects of individual atoms can dominate the behavior of materials at the nanoscale. In this way, accurate physical insights can be reduced at the atomic level under conditions that cannot easily be observed experimentally. Direct manipulation of the nanostructure is complex[51].

There are two main groups of methods in computational studies: dynamic and static. Dynamic methods consider the interaction between atoms purely dynamic. Dynamic methods are sub-classified into three main categories: classical molecular dynamics (MD), Monte Carlo (MC), and ab initio. On the other side, the static methods simplify the atomic interaction to static behavior. They are subdivided into two main types: molecular mechanics (MM) methods and continuum shell methods. The computational resource selection will be coupled with appropriate methods depending on the study of interest. In particular, the methods of molecular modeling and molecular dynamics capture structural aspects of the interaction and morphology developed between nanostructures and biological molecules or polymers in a shorter time than either ab into. Among the nanostructures used for biomedical applications, large carbon nanotubes represent a particular case of study given their chemical structure and well-known surface topography[51,52].More details on molecular dynamics will be given in the methodology section.

In summary of chapter, Nanotechnology through the merging of nps with medicine presents an unprecedented opportunity for developing novel materials that can significantly improve treatment and diagnosis of diseases. The small size and large surface area of nanomaterials facilitate the creation of supports and accessories for implants and provide an excellent specific therapeutic effect. Therefore, biomaterials can improve the quality of medical procedures benefiting both the patient and the health personnel. Within the field of materials nanotechnology, carbon nanostructures are being studied with great interest. Among the existing carbon nanostructures, carbon nanotubes stand out due to their remarkable physical properties and chemical stability, previously mentioned in this document. In biomedicine, CNTs present friendly support for the biological substrate and act as a specific partner in biochemical interactions and the miniaturization of medical devices. CNTs are used to develop biosensors, drug delivery systems, implants, tissue regeneration, and others. However, their application in the biomedical field requires considering possible toxicity problems when using them as free radicals or achieving good dispersion of CNT in solvents (especially in water). In recent years, scientists have focused on the functionalization or coating of the surface of nanotubes with polymers to overcome toxicity problems. This polymer/CNT interaction can modify the properties of the CNT surface and ultimately lead to a change in their biological behavior and impact on their biodistribution. Each polymer behaves differently in the presence of the nanotube due to the functional groups that make it up or their concentration. Therefore, it is essential to have a proper understanding of the atomistic interaction of a polymer with the surface of CNTs to engineer novel nanoscale devices and materials. One approach that can provide accurate atomistic-level information regardless of the experimental challenges of studying the materials is through computational simulations. This means that through computational studies, it is possible to have a thorough knowledge of the physical, mechanical, and surface properties of materials at the microscopic and/or atomic levels. This way, the payload for experimentation can be reduced, and accurate physical insights at the atomic level where experiments are not feasible can also be provided. Therefore, given the current relevance of polymer/CNT-based biomaterials and their wide range of applications, the present work focuses on studying the superficial interaction between polyvinylpyrrolidone and multilayer carbon nanotubes throughout molecular dynamic simulations. In the following section, the objectives proposed for the development of this research are detailed.

1.5 Objectives

General Objetive

The general objective is to perform a detailed description of the behavior of one or several PVP polymers in the presence of a carbon nanotube through the computer simulation method of molecular dynamics.

Specific Objectives

- To generate two representative atomic models of CNT types: an SWCNT and a representative model of MWCNT and, identify structural differences between them.
- To describe the adsorption and structural interaction between PVP and both CNT models through the analysis of molecular dynamics simulations.
- To determine the influence of the concentration of PVP polymers on the adsorption dynamics over each CNT surface model.

Chapter 2

Methodology

2.1 Molecular Dynamics

The computational methodologies of molecular dynamics provide valuable information to understand the functioning and the atomic-level mechanisms of diverse molecular systems.MD methods treat the atoms as classical entities (position and momentum). They are based on Newton's second law or the equation of motion, depending on the force exerted on the atom (mass and acceleration) .From this trajectory, the average values of properties can be determined. Once the positions and velocities of each atom are known, the state of the system can be predicted at any time. Inter-atomic potentials are the core of classical MD methods and there is no explicit consideration for the electrons[51]. The treatment of atoms and their bonds is defined by a force field, in which each sphere or atom is assigned a type depending on its charge, its hybridization, and bonds. Each type of atom has parameters such as force constants, radius, and mass. These parameters are obtained mainly through experimental values or calculations at the level of quantum mechanics.

Over the years, multiple force fields have been developed such as AMBER[53], CHARMM[54], OPLS, GROMACS[55], and COMPASS[56] depending on the molecular systems in study: for biological macromolecules (proteins, RNA, ,small organic molecules or inorganic systems. Each force field is characterized by the definition of a potential energy equation, which allows obtaining an approximation of the energy of a molecule in the state in which it is. Below are some standard terms among the force fields, understanding that each field defines its equation by adding elements and modifications to better approximate the energy of the molecular system[57].

i.Bonding interactions: Model mathematically the intramolecular behavior of bonds, bond angles, dihedral angles, and torsional angles. For this purpose, quadratic harmonic potentials, and periodic functions, among others, are used. Internal coordinate effects are included in some force fields, combining some parameters called cross-terms, such as bond-angle and angle-angle.

ii. Non-bonding interactions: Include the effects of intermolecular interactions described by Coulomb's laws. The interactions are calculated by the partial charges assigned to each atom and Van der Waals interactions, commonly modeled by Lennard-Jones electrostatic potentials.

Energy minimization is based on searching for solutions to the potential energy equation, a space called the potential energy surface. The stationary states have zero derivatives concerning the coordinates. Such states correspond to the system's steady states and are known as energetic minima. In these states, we find local and global minima. The former are commonly explored by derivative or gradient methods as conjugate gradients and steepest gradients. The latter is explored by stochastic methods such as Monte Carlo, Simulated Annealing, and other evolutionary algorithms.Energy optimization is usually applied as a preliminary step to simulation studies. Molecular dynamics generate a set of representative configurations that derive structural and thermodynamic properties. Dynamic molecules studies the system's behavior as a function of time, generating a trajectory by integrating Newton's equation of motion for each atom[58].

$$\frac{\delta^2 r_i(t)}{\delta t^2} m_i = F_i \tag{2.1}$$

where, m is the mass of particle i, r is the position and t the time. F represents the force that acts in the particles system, obtaining the energy potential gradient, such that:

$$F_i = -\nabla U(r_1, ...r_n) = -(\frac{\partial U}{\partial x_i}, \frac{\partial U}{\partial y_i}, \frac{\partial U}{\partial z_i}) \tag{2.2}$$

where $U(r_1, ...r_n)$ describes potential energy of n particles that are interacting with a force field. Due to the dependency of multiple atomic coordinates of 2.2 it is solved by numeric integration. The Verlet algorithm is a numeric integration method that is based in Taylor series expansions in terms of the positions $r_i(t)$[59].

$$r_i(t + \Delta t) \cong 2r_i(t) - r_i(t - \Delta t) + \frac{F_i(t)}{m_i} \Delta t^2 \tag{2.3}$$

In practice, the term Δt is known as time step and is determined by minimum motions of the system, such as the vibration of bonds in light atoms (O-H, C-H) and is generally in the order of femtoseconds to ensure stability in the numerical solutions obtained. In the previous equation a current state depends on a previous state, which implies that molecular dynamics is a deterministic method.

An important aspect of molecular dynamics is its connection with statistical mechanics because the conformations (microstates) accessible to the system compose what is known as phase space. This 6N-dimensional space comprises the 3N coordinates and 3N momenta of a system of N atoms. Based on the ergodic hypothesis, it is possible to calculate macroscopic properties through a representative average of microstates called a collective or ensemble. Each ensemble is characterized according to which thermodynamic properties are employed in the systems, either in particle number (N), chemical potential (μ), volume (V), pressure (p), energy (E), or temperature (T), defining each thermodynamic state by giving value to three of the variables mentioned above. The most well-known assemblies are the following:

- (N, V, E) Microcanonical ensemble
- (N, V, T) Ensamble Canónico
- (μ, V, T) Grand canonical ensemble

- (N, p, T) Isothermal-isobaric ensemble

To define the initial state of a molecular dynamics, either an experimentally derived structure or an energetically optimized structure is used. Then, initial velocities are randomly assigned so that they behave according to a Maxwell-Boltzmann distribution under a certain temperature. Subsequently, properties such as potential, kinetic or total energy, temperature, pressure, etc. are evaluated until stabilization, a stage called equilibration phase. Finally, with stable properties, the phase space is sampled and macroscopic properties of interest are calculated, a stage known as the production stage.

2.2 Input and Output Files

The following is a brief description of the types of input and output files to be used in the modeling and simulations of this study. The files mentioned refer to the visualization and simulation programs that we have chosen to realize this work. Therefore, the description of each file has been obtained from the NAMD user's manual[60]. However, most of the files to be mentioned are adapted to different molecular dynamics programs.

- PBD files (coordinate file): The PDB (Protein Data Bank) format is used for coordinate data of the protein or polymer and any waters, ions, or other heterogeneous atoms in the crystal being read or written for most molecular dynamics programs as well, NAMD, X-PLOR and CHARMM. The file mainly includes the record type, atom ID, atom name, residue name, residue ID, x, y, z coordinates, segment name, and line number. Due to the limits of x-ray crystallography and NMR structure analysis, the coordinates of hydrogen atoms are not included in the PDB.
- PSF files (Protein Structure File) : This file contains the molecule-specific information needed to apply a particular force field to a molecular system. The PSF file contains six main sections of interest: atoms, bonds, angles, dihedrals, impropers (dihedral force terms used to maintain planarity), and cross-terms. SF files may be in either CHARMM or X-PLOR format. Hydrogen atoms are included.
- CHARMM parameter files: The CHARMM force field is divided into a topology file, which is needed to generate the PSF file, and a parameter file, which supplies specific numerical values for the generic CHARMM potential function:
    - The topology file (.rtf file) contains all of the information needed to convert a list of residue names into a complete PSF file. Additionally, It contains internal coordinates that allow the automatic assignment of coordinates to hydrogens and other atoms missing from a crystal PDB file. Basically, defines the atom types used in the force field; the atom names, types, bonds, and partial charges of each residue type; and any patches necessary to link or otherwise mutate these basic residues.
    - The parameter file (.prm file) : A parameter file contains all of the numerical constants needed to evaluate forces and energies, given a PSF structure file and atomic coordinates. It provides a mapping between bonded and nonbonded interactions involving the various combinations of atom types found in

the topology file and specific spring constants and similar parameters for all of the bond, angle, dihedral, improper, and Van der Waals terms in the CHARMM potential function.

- NAMD Configuration Files (.conf file, or .namd file) : This file specifies what dynamic options and values NAMD should use, such as the number of timesteps to perform, initial temperature, etc. The options and values in this file control how the system will be simulated. It is given to NAMD on the command line and specifies virtually everything about the simulation to be done.
- Output NAMD files :At the end of every simulation, NAMD writes different files containing important information such as final coordinates (output.coor), final velocities (output.vel), restart information (.restart), coordinate position trajectory (.dcd), and others. These files are helpful for visualization and analysis of simulation results

2.3 Modeling of molecular structures : PVP and CNTs models

One of the significant challenges of simulating multilayer carbon nanotubes is the considerable computational cost required due to the excessive number of atoms involved in their structure. Therefore, a simplified 3-layer graphene model is presented in this project to understand the relevance of interlayer interactions in the study of the surface interaction of the model with the polymer. In addition, a single-wall carbon nanotube is presented as a close approximation of a tubular model. Both systems will be exposed to the same calculations and analysis.

PVP and SWCNTs structures were built using CHARMM-GUI, a web-based graphical tool to interactively build complex systems and prepare their inputs with well-established and reproducible simulation protocols for molecular simulations. The molecular model of SWCNT is shown in (Figure 2.1a). SWCNT models preset a zigzag chirality of 7.8Å and a length of 52Å. The basic repeat unit and a single chain of the PVP are illustrated in (Figure 2.1b).The single chain of PVP consists of 30 repeat units (monomers), giving a length of 80Å. Finally, a three-layer flat graphene surface (Figure 2.1c) represents a large MWCNT to reach a reasonable simulation time and statistics. The three layers were individually constructed and then combined into a single system at a distance of 3.4Å from each other. The C-C bonds in the graphene layers correspond to 1.41Å as in the SWCNT systems.

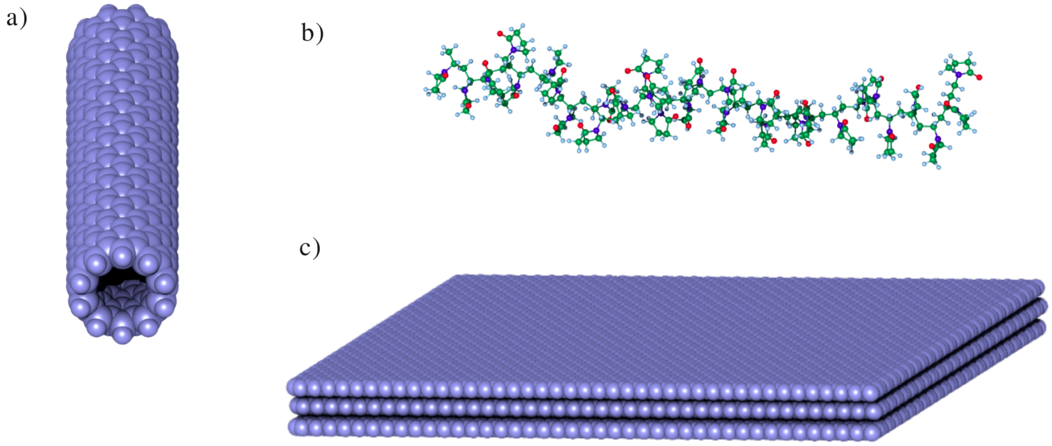

Figure 2.1: Molecular structures of the proposed models. a) model of a SWCNT; b) model of PVP composed of 30 monomers; c) model of a 3-layer planar graphene.

Visual Molecular Dynamics (VMD)[61] was used to build the graphene model mentioned above. It is a molecular visualization program that displays, animates, and analyzes large bio-molecular systems using 3D graphics and built in scripting. Additionally, this program will be used to design all the systems to be simulated because of its ability to act as a graphical front end for an external MD program by displaying and animating a molecule undergoing simulation on a remote computer[62].Figure 2.2 describes the process in more detail.

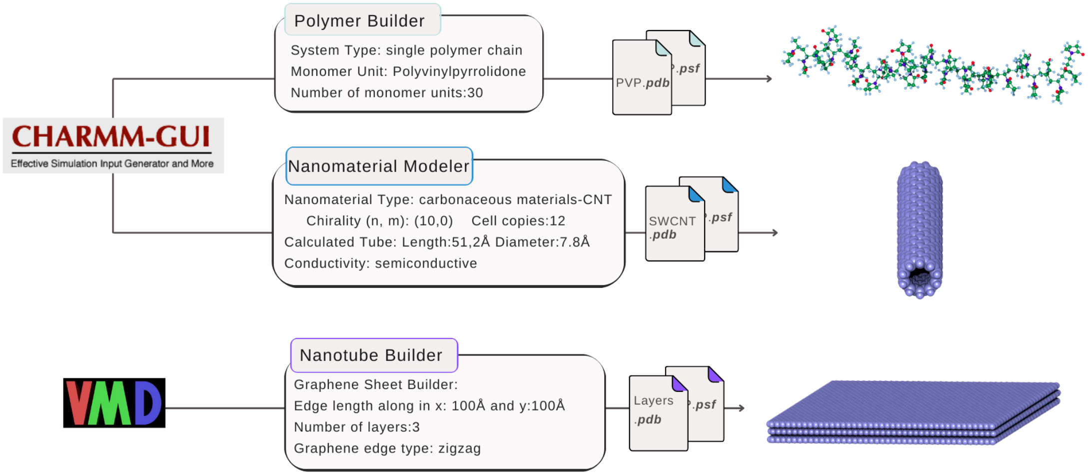

Figure 2.2: Schematic representation of modeling the atomic structures process. In the present scheme, the CHARMM-GUI software allows the molecular structure built of PVP and SWCNT through specific software tools. The PVP was obtained through the Polymer Builder, while the Nanomaterial Modeler tool was used to build the SWCNT. On the other hand, the nanotube builder tool of the VMD software allowed the construction of the graphene layers. Both CHARMM-GUI and VMD were provided with the required construction parameters. Two output files were obtained for each molecular structure: structure file (.psf) and coordinate file (.pdb).

2.4 PVP-SWCNT system construction

In the present study, two based systems were built: PVP-SWCNT and PVP-MWCNT. The PVP-SWCNT system consists of a unit of SWCNT and a single chain of PVP. The distance between the SWCNT and polymer chain was initially 15Å to give the polymer as much conformational freedom as possible before being influenced by the CNT. Then, the PVP chain and the SWCNT system were inserted into a periodic water box of 85x85x110Å^3 and centered on the Z-axis. Subsequently, the corresponding ions were added for the neutralization of the system. The result systems are present in (Figure 2.3).

The MWCNT representative system includes a PVP chain at 15Å of the periodic graphene surface of 100x100Å The system was inserted in a 100x100x80Å^3 periodical water box corresponding to the x,y, and z-axis dimensions. Then, the system was neutralized with sodium ions. In addition, positional restraint was applied in the MWCNT model (middle layer) to avoid vertical movement of the graphite layers; on the other hand, no restraints were applied to the SWCNT, which due to the periodic conditions, remains aligned to the z-axis, thus facilitating the subsequent analysis. The periodic boundary conditions are employed to eliminate the effect of the small size system and surface effect and mimic the infinite bulk surrounding the N particles system. The application of periodic boundary conditions helps in minimizing the edge effects. Under this scheme, atoms are packed into a space-filling box surrounded by translated copies of itself, which imposes no boundary condition. A particle can interact with its neighboring particles in the infinite system rather than in a finite system.

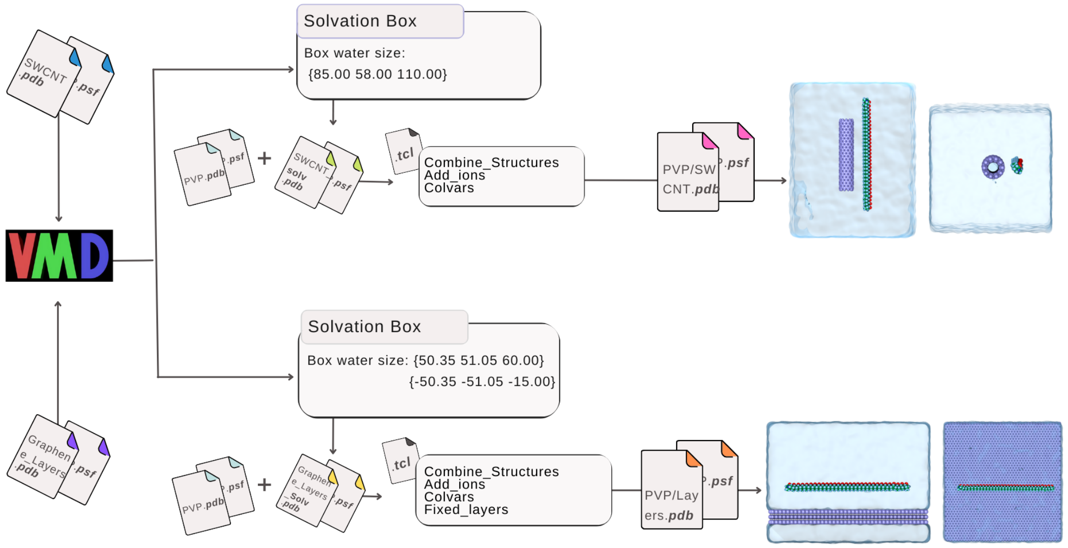

Figure 2.3: Schematic representation of the construction of the PVP/SWCNT and PVP/graphene layers. From the psf and pdb files obtained in modeling the structures, we proceeded to solvate them in a water box large enough to cover the structures and allow free movement. Then, the psf and pdb files of the PVP with the psf and psd files obtained from the solvation were exposed to a set of processes to combine and stabilize the structures inside the water box. Thus, the final files for the simulation are obtained. The exact process is performed for the CNT single wall model and the graphene layers.

2.5 Molecular dynamics simulations

Once the systems have been built, the simulation process can begin. This process consists of three main stages: initiation, minimization, and production. Each stage is briefly detailed below, and (Figure 2.4) shows a graphical representation of them. The molecular dynamic simulation process is carried out in the NAMD software, a parallelizable molecular dynamics software designed for high-throughput simulation of large biomolecular systems[63].

- Initialization (structure, topology, and force field files): The input files are needed to start the simulations. In this case, the files for $SWCNT - PVP$ systems are structure file $SWCNT10\_1pvp30\_fina.psf$ and the coordinate file $SWCNT10\_1pvp30\_final.pdb$ while for the $Layer - PVP$ systems the needed files are structure file *layer_1pvp30_fina.psf* and the coordinate file *layer_1pvp30_final.pdb*. These files were obtained in the previous step (2.3). The parameter files to use are *par_all36_prot_lipid_water_ions.prm*, *toppar_all36_synthetic_polymer.str*, *par_all36_cgenff.prm* from CHARMM force field.

- Energy minimization: The purpose of this stage is not to find a valid global energy minimum but to adjust the structure to the force field, and particular distribution of solvent molecules and to relax possible steric clashes created by guessing the coordinates of atoms during the generation of psf file.

- Molecular dynamic simulation in NPT ensemble: In an NPT ensemble, the number of particles N, pressure P, and temperature T are kept constant. The unit cell vectors are allowed to change, and the pressure is adjusted by adjusting the volume. This ensemble is also called the "isothermal-isobaric" ensemble and usually closely resembles experimental conditions. The production stage involves an NPT ensemble using Langevin thermostat, Langevin piston barostat[64], and 4fs time-stepping[65] via NAMD 2.13 software. In the first part of the simulation, the polymer finds a stable conformation and comes in contact with the surface. Once stable, the data we will use in the analysis begins to be produced. In total, each system had a simulation time of 100ns. Each simulation took an average of 75 hours with 12 CPUs and a graphics card. The computational resources were provided by the nano-biomaterials research group of Professor Horacio Poblete at the University of Talca, Chile.

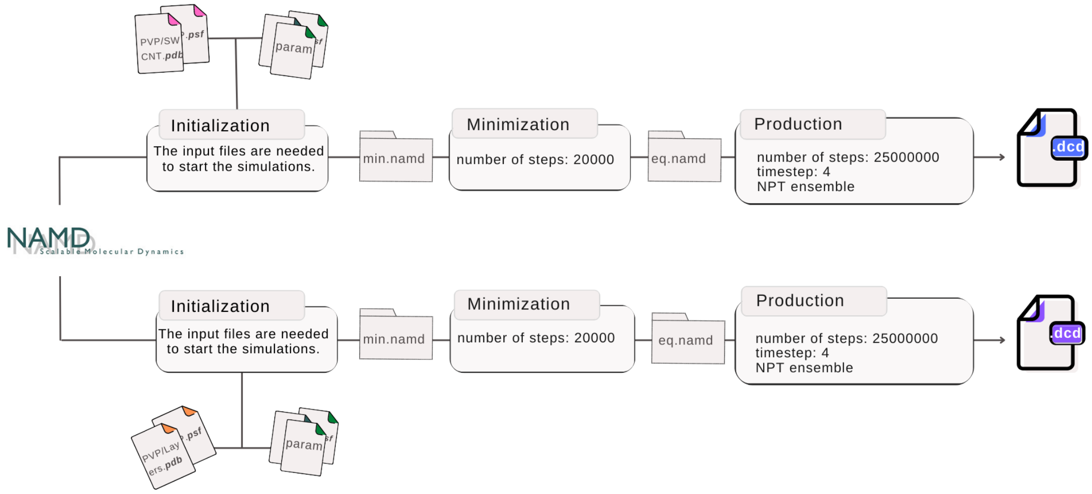

Figure 2.4: Schematic representation of the system simulation stages. The scheme shows three stages of simulation processes: initialization, minimization and processing. These processes are performed through the NAMD software. It requires the input of namd files (initialization) for both minimization and processing. These namd files contain the psf and pdb files of the systems and parameters along with a set of specifications for the performance of each process. When the minimization is done, the simulation can continue with the processing. Finally, a series of files is obtained, including the file of atomic coordinates over multiple frames time-steps.

Chapter 3

Results & Discussion

This study considered two representations of CNTs: a single-walled carbon nanotube model and a three-layer graphene model. These models were chosen because of the complexity and excessive simulation time required for a large multilayer model. On the one hand, the single-layer model allows analyzing the interaction of PVP in a tubular structure. On the other hand, the 3-layer graphene surface enables an understanding of the PVP interaction in a larger area influenced by interlayer forces. In both models, Five different concentrations of PVP were used in the modeling of systems (see tables: 3.1 and 3.2). The amount of PVP varied from 1 polymer up to an amount of 20 polymers. These systems are shown in figure 3.1

Table 3.1: SWCNT models

Model	No. of CNTs	No. of PVP polymers	% No. of water molecules	Surface area of CNT($\AA^3$)
SWCNT:1	1	1	24996	199.68
SWCNT:5	1	5	24546	199.68
SWCNT:10	1	10	24055	199.68
SWCNT:15	1	15	23486	199.68
SWCNT:20	1	20	22996	199.68

Table 3.2: Graphene layer models

Model	No. of CNTs	No. of PVP polymers	% No. of water molecules	Surface area of CNT($\AA^3$)
Layer:1	1	1	20595	10281.47
Layer:5	1	5	20188	10281.47
Layer:10	1	10	19663	10281.47
Layer:15	1	15	19145	10281.47
Layer:20	1	20	18565	10281.47

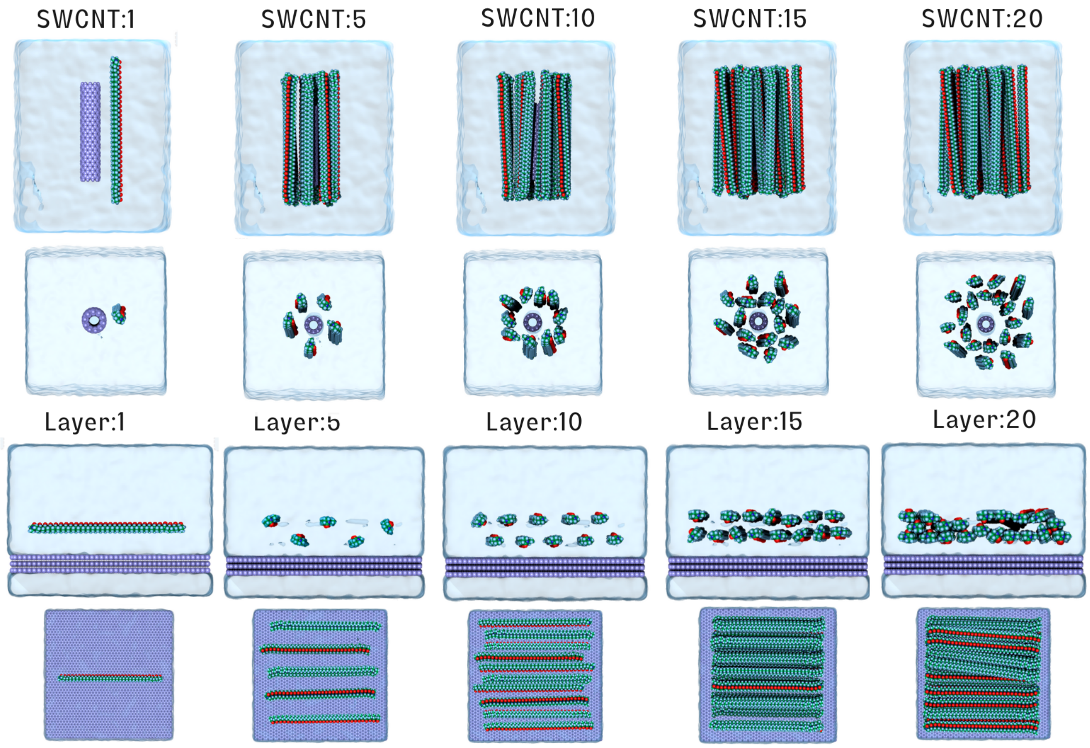

Figure 3.1: Graphical representation of the systems generated for two models of CNTs: SWCNT and graphene layers.The systems presented differ in the amount of polymer in the system.

3.1 Surface interaction of CNT models

In the first instance, only systems composed of one PVP polymer chain were analyzed to know in detail the behavior of PVP on CNTs without the influence of other PVP chains. In addition, each analysis was performed under the same conditions as the two proposed CNTs models to understand the influence of PVP interaction with single-layer nanotubes and multilayer nanotubes.

3.1.1 Dynamics of CNTs systems

Simulations of the SWCNT:1 system show the first approach of the PVP to the SWCNT in the first nanosecond of simulation. A few nanoseconds later, it adopts an enveloping conformation over the system and stays close to it despite the constant movement of the SWCNT through the system. In detail, (Figure 3.2) shows how the PVP bends to fit along the surface of the CNT and maintains that confirmation throughout the simulation time (100ns). The wrapping of polymers on the surface of CNTs is a general phenomenon of water-soluble polymers such as PVP. due to the weak non-covalent interaction (CH-π and Van der Waals forces) to serve as the driving force to stimulate the spontaneous wrapping[66]. This agrees with previous experimental and computational investigations of SWCNT with PVP or similar polymers. For instance, O'Connell et al. presented the solubilization of SWCNT in water by non-covalently association with linear polymers, most successfully with PVP and polystyrene sulfonate (PSS). These results are strong evidence that the polymer and SWCNT comprise a single entity that can be manipulated as a whole. They conclude that helical wrapping geometries maximize the number of polymer units interacting with the nanotube surface, increasing polymer chain length at the expense of some torsional energy. Also, their AFM studies show a uniform diameter along their lengths with heights consistent with monolayer coverage of the SWCNTs, supporting the interpretation that the polymer is uniformly wrapped around the tubes rather than associated with the side walls at various points as a random coil[67]. Similarly, Zheng et al. observed molecular interaction between SWCNT and polyethylene/ polypropylene/ polystyrene/ polyaniline molecules. The computational systems prepared with each polymer tended to wrap around the nanotube[68] .

In the case of the layer:1 system (see also Figure 3.2), the layers are fixed during the simulation. In the first nanoseconds, the PVP begins to approach the graphene layers, similar to the SWCNT model behavior. Furthermore, it is observed that not all monomers interact simultaneously with the surfaces. This differs from the SWCNT system, where the PVP wraps to the surface, allowing more monomers to interact with the tube surface (Figure 3.2). The size of the polymer directly influences this behavior compared to the graphene layers and the fact that the layers are fixed in the same position throughout the simulation. Therefore, it is not possible to visualize any wrapping on the sides of the layers due to the imposed periodic boundary conditions, which generate an infinite surface in the XY-plan. However, related researchers show that for MWCNTs, there is also a warping effect with PVP. Huang et al. discuss different principles of interaction between MWCNTs and dispersing surfactants in their work. They mention that with a stable MWCNT-PVP dispersion, the macromolecular chains of the nonionic surfactant are predicted to wrap around the MWCNT surface, preventing the aggregation of MWCNTs and forming a stable dispersion with water[69]. The polymer wrapping of CNTs represents an actual result in PVP-CNT interaction to improve the dispersion of CNT into a matrix of composites and the possibility of manipulating and organizing the CNT into ordered structures. Huang et al. reported a series of MWCNT-surfactant dispersion experiments where the most stable MWCNT dispersion in water was obtained using PVP to wrap around the MWCNT, preventing agglomeration. They suggest that the higher ability of long chains to suspend nanotubes is attributed to enhanced steric stabilization of the large-sized hydrophilic groups grafted along the flexible backbone wrapped around the nanotubes[69].

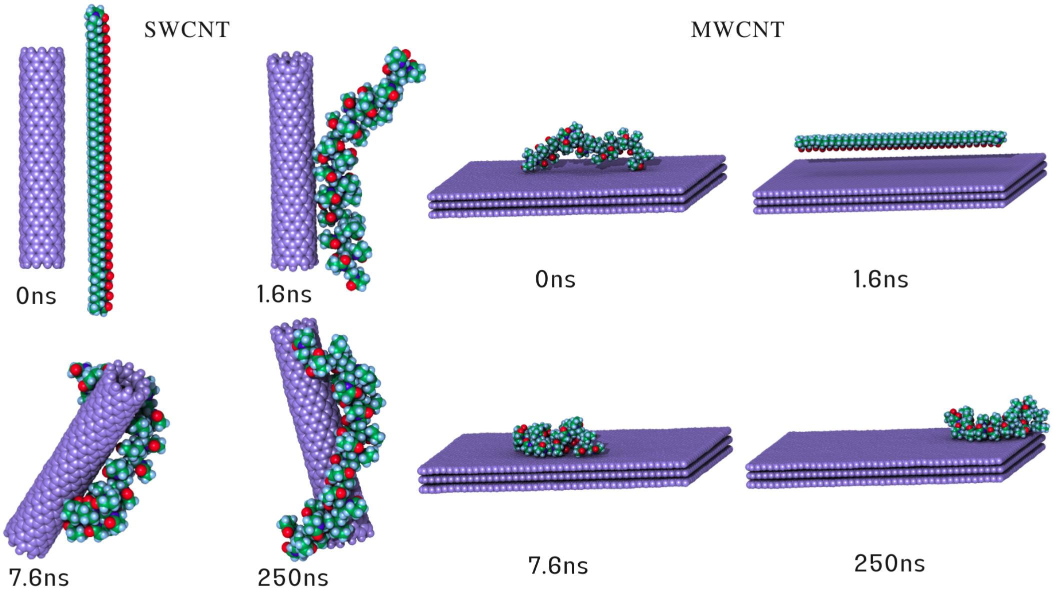

Figure 3.2: Different stages of the simulation of the SWCNT:1 and Layers:1 systems. 0ns: initial configuration with the nanotube; 1.6ns: start of polymer-surface interaction; 7.6ns: total coupling of the polymer on the surface; 250ns: representation of the overall behavior of the PVP on the surface throughout the simulation. Each stage event occurred at similar times (less than one ns difference) in the exposed systems.

3.1.2 CNTs surface covered by PVP and atoms involved

After the evidence of the close approximation of the PVP to CNT models shown in the dynamics of the systems, the number of PVP monomers on the surface was calculated to determine the percentage coverage. It is observed that both the SWCNT system and the layered system exhibit 14 monomers with at least one atom at 4Å of the nanotube surface. In the SWCNT:1 system, the PVP monomer occupied 0.28nm^2 of surface area, and the total coverage was 24.54%. In comparison, the surface coverage of graphene layers reached 5.21% of the total area, with coverage per molecule of 0.03nm^2. It should be emphasized that the area of SWCNT is less than the area of the layered model. So even though the PVP polymer used in each system is the same, we can notice that the 14 interacting monomers represent a higher area coverage for the SWCNT model than for the layered model.

Next, the critical atoms related to the interaction were identified for a deep analysis of the superficial behavior. The distribution of distance of PVP atoms to the surface of the CNT models was analyzed. In detail, (Figure 3.3a)

Table 3.3: Graphene-layers

Total PVP in the system	PVP-CNT	Monomers-CNT	coverage	molnm^2
1	1	14 ± 1.62	535.34 ± 22.43	0.03 ± 0.00
5	5	78 ± 9.25	2849.57 ± 56.49	0.027 ± 0.00
10	10	149 ± 20.64	5191.45 ± 82.52	0.028 ± 0.00
15	13	127 ± 14.54	4646.36 ± 75.23	0.027 ± 0.00
20	10	145 ± 12.24	4980.33 ± 66.47	0.029 ± 0.00

Table 3.4: SWCNT

Total PVP in the system	PVP-CNT	Monomers-CNT	coverage	molnm^2
1	1	14 ± 1.70	49.02 ± 3.65	0.29 ± 0.02
5	5	49 ± 3.61	179.76 ± 4.2	0.31 ± 0.01
10	10	48 ± 9.47	142.60 ± 5.13	0.34 ± 0.01
15	13	61 ± 4.78	164.00 ± 4.22	0.37 ± 0.01
20	10	48 ± 7.17	150.34 ± 4.91	0.32 ± 0.01

shows a model of the PVP molecule, highlighting in red, blue, green, and gray the atoms Oxygen (O), Nitrogen (N), Carbon (C), and Hydrogen (H), respectively. At the same time, (Figure 3.3b and3.3c) show the distance distribution of these atoms on the surface of CNT models. In the SWCNT:1 system, it should be noted that the present distance distribution considers the PVP interacting with the SWCNT and the periodic images of the SWCNT because it is not fixed in a particular position. This results in more considerable distances between the PVP atoms and the SWCNT. However, the results display a closer distance (between 2Å to 3Å) of Hydrogen atoms to the SWCNT surface; meanwhile, the C, N, and O atoms show similar distributions among them, with a higher probability of finding these atoms at distances higher than 4Å from the SWCNT surface. On the other hand, the atomic-distance distributions on the MWCNT surface show that all atoms involved interact closely with the surface throughout the simulation. However, hydrogen atoms are more likely to show shorter distances (less than 3Å) than other atoms. The distance distribution peaks for both cases (SWCNT and Layer) suggest that CNTs naturally interact with the polymer chains through Van der Waals and slightly non-bonding electrostatic forces. Studies such as Georgakilas et al. mentioned that the non-covalent functionalization is principle-based in Van der Waals as polymers present a hydrophobic part while ionic interactions and hydrogen bonds are related to the presence of oxygenated groups on the CNT surface[70]. Manivanna et al. suggest that the absence of an electronegative atom in SWNTs nullifies the possibility of forming

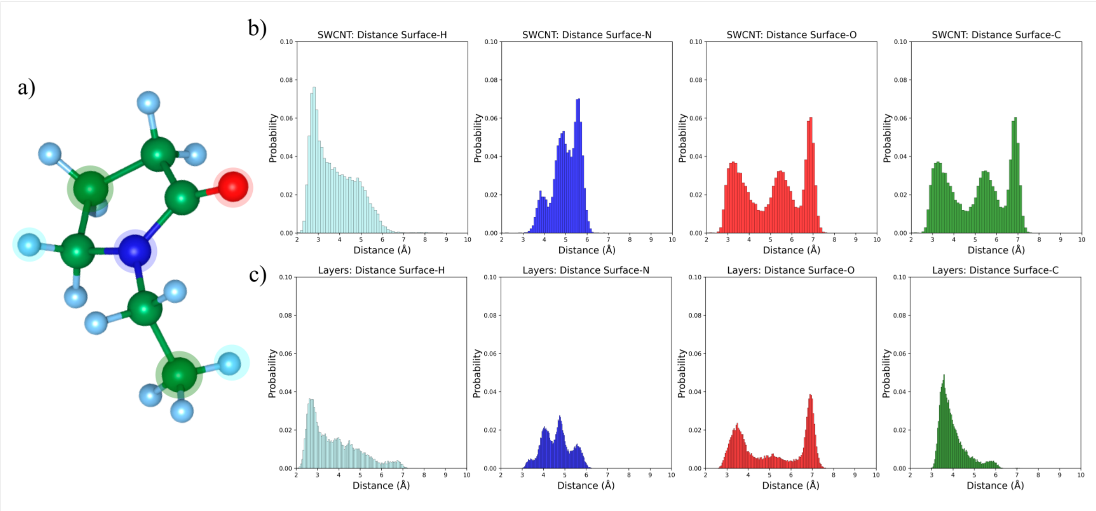

Figure 3.3: Polyvinylpyrrolidone atomic-distance distributions in 1:1 complexes in CNT models. A) Representative scheme of PVP molecule, showing atoms C5, O1, N1, and H51 (green, red, blue, and gray respectively). B) Distribution of distance probability of key atoms of PVP from SWCNT surface. C) Distribution of distance probability of key atoms of PVP from graphene layers surface. The distances are averaged over 100ns of simulation

H-bonds with PVP so that the enveloping functionalization occurs through Van der Waals interaction[71].

Finally, the distance of H atoms less than 3Å to the CNT surface was calculated within the range of bonding distances in non-covalent interactions. The hydrogen atoms of PVP presented an average of 2.41Å to the SWCNT. At the same time, PVP shows a distance of 2.73Å to the surface of the graphene layers. The difference in the average distance between both systems is due to Van der Waals forces between the graphene layers, making the interaction with hydrogen or any other atom in the polymer less strong than the interaction of the single-layer nanotube. This is in agreement with research by lee et al. in which they compared single-layer and bilayer graphene layer models, respectively, to evaluate the relevance of Van der Waals forces on the interaction of graphene with molecules on the surface. They mention that the interaction between graphene layers decreases the buckling and deformations in the top graphene sheet when a molecule is deposited. In other words, they affect the top graphene layer's chemical reactivity, which is a significant factor in the chemical stability of graphene. This phenomenon is evidenced and has great reactive affectation in covalent functionalizations[72]. However, it can be evidenced to a lesser extent in electrostatic interactions, as in (Figure 3.4). The SWCNT model shows more significant lattice deformation than the graphene later models, where the minor perturbation is evidenced in the bond sizes of the C atoms on the surfaces of the models.

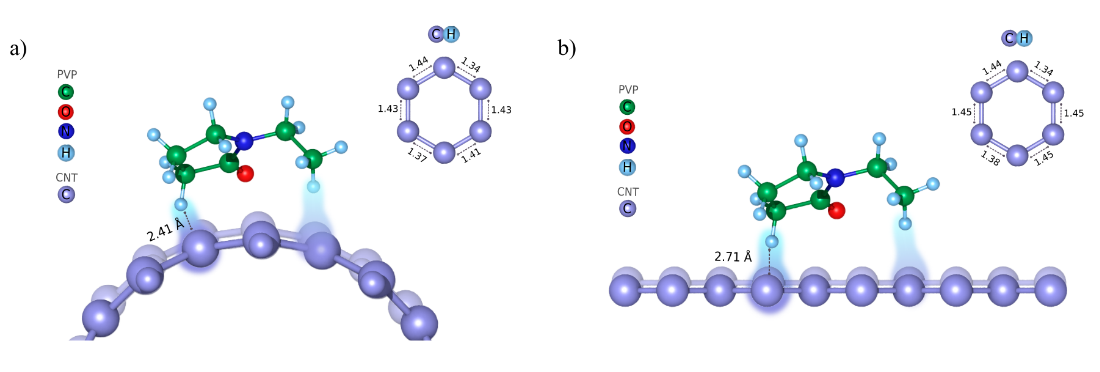

Figure 3.4: Interaction of PVP hydrogen atoms with CNTs models. (a) and (b) show the interplay between the hydrogen atoms of PVP on the surfaces of the studied models (SWCNT and graphene layers respective).

3.2 PVP-CNT interaction based on influence of PVP concentration

The following is the analysis of the influence of the amount of polymer in the general dynamics of the system and the interaction of the same on the surface of the CNT models. The behavior of PVP in the system is described as the number of polymers increases. The surface area covered in each system is detailed, and finally, the distance distribution between the PVP atoms and the CNT surface is analyzed. The amount of PVP used in this study was 5,10,15, and 20 polymers. The dynamic behavior at 100ns figure 3.5 of the SWCNT systems shows agglomeration of the PVP around the carbon nanotube, and the polymers that fail to interact directly with the surface begin to polymerize around it, forming a PVP coating. This represents in the distribution graph (Figure 3.5b) an increase in the distances between the PVP and SWCNT due to the amount of polymer compared to the SWCNT surface.

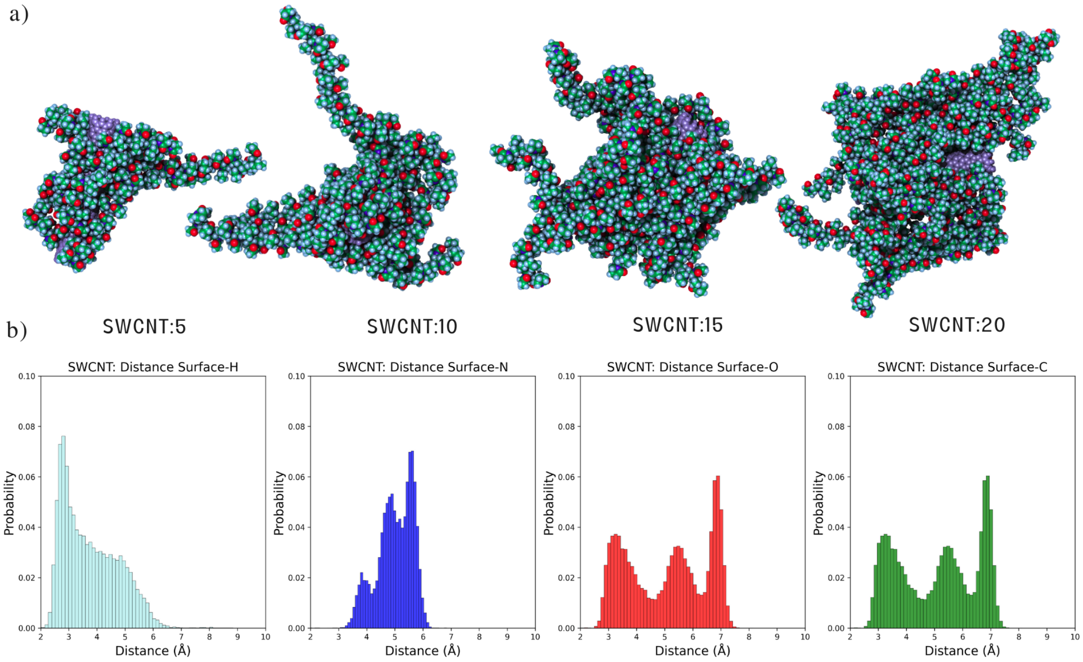

Figure 3.5: PVP behavior and distribution distance probability of atoms of PVP form SWCNT surfaces models in 1:5, 1:10, 1:15, 1:20.

Among these, the highest coverage of SWCNT surface can be seen for the system with five polymers of PVP. This system is the only one in which the totality of the arranged PVP interacts with the surfaces presenting 49 monomers. Similarly, the SWCNT:10 system showed 48 interacting monomers. However, the area covered per molecule is lower than that of SWCNT:5. Thus, there were a more significant number of interacting polymers. The total area covered did not exceed 142.6, representing 71.41% coverage. This was the system with the lowest percentage of coverage and the most outstanding dispersion of results. Similarly, the SWCNT:20 system presents 48 monomers with a standard deviation of 7.17. In this case, the area per molecule is greater than in the SWCNT:5 system despite having a similar number of interacting monomers. The higher standard variation may influence this difference in total coverage in PVP monomers, and each molecule in SWCNT:20 occupies less nm^2 than the molecules in the SWCNT:5 system. On the other hand, the SWCNT:15 system presents seven interacting polymers with an average of 61 interacting monomers. It also shows $0.027nm^2$ of coverage per molecule. Thus, the system with the least coverage per molecule, despite having the highest number of interacting polymers, has coverage of 82.13%, which is 10% lower than the 5-polymer PVP system. It can be assumed from the interaction result that six polymers of PVP are an ideal amount for covering the total surface of an SWCNT with an area of $199.68A^3$. In addition, as more PVP chains are added to the surface, they interact with each other producing a kind of coverage that will be more forceful as more PVP is added.

On the other hand, in the graphene surface models, we can observe a sufficient surface area for the higher polymer concentration system to interact fully with the graphene surface. However, any system is completely covered (see Fig 3.6). It can be observed that the 20 PVP-graphene layer system achieves coverage of 48.43% on the graphene surface. This is lower than the percentage of coverage achieved by the system composed of 10 PVP polymers. Although there is enough space for the polymers to interact with the entire surface, the polymers prefer to interact with each other. Therefore, it can be noted that there is an influence of PVP concentration on the behavior of PVP on the surface of both SWCNT and graphene layers. Thus, in general, the interaction of PVP with CNTs at low amounts allows the PVP to wrap around the surface, while at higher concentrations of PVP on the surface, it produces a coating around the PVP.

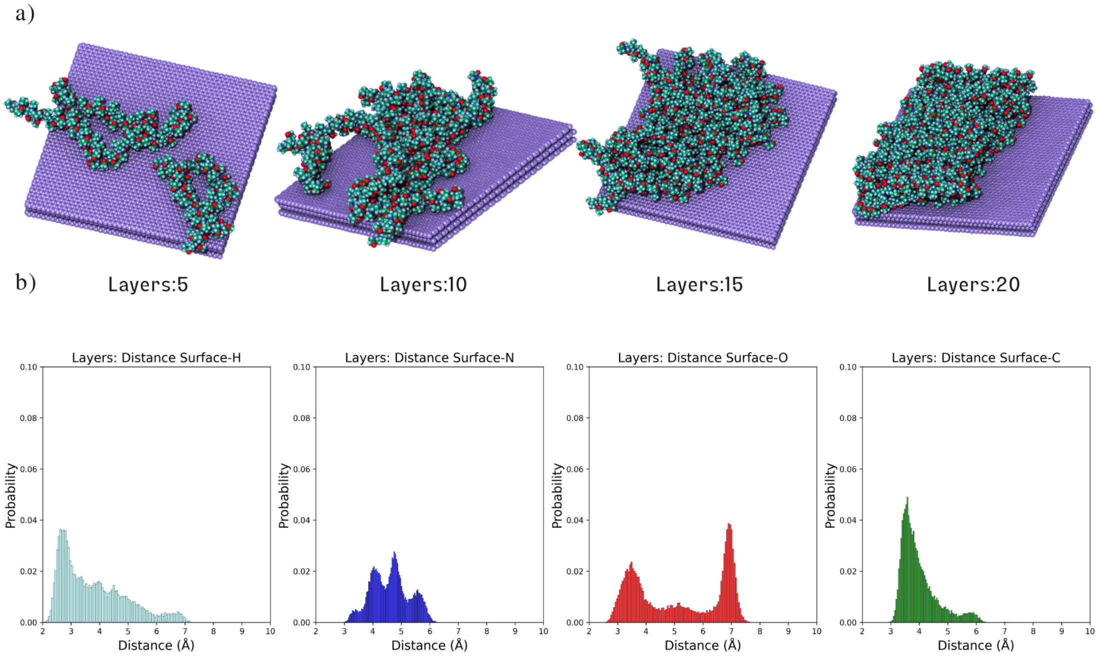

Figure 3.6: PVP behavior and distribution distance probability of atoms of PVP form graphene layers surfaces models in 1:5, 1:10, 1:15, 1:20.

Thus, the amount of PVP used in the system influences how it interacts with the carbon nanotube, which can influence the performance of the composite. Samanta et al. suggest that only a polymer chain of a certain length can achieve a homogeneous dispersion of nanotubes in the polymer matrix through their study of bundling and dispersion of SWNT by flexible conjugated polymers such as PFx and P3AT. Their result confirms that polyfluorenes with an alkyl chain length of eight carbons effectively disperse SWNTs of diameter 0.8-1.2 nm, and longer alkyl chains with 12-15 carbons are favored for the dispersion of nanotubes of increased diameter up to 1.5 nm. While Salazar-Rios et al. mentioned that the CNT length also has relevance in the interaction with a determined polymer. They analyzed the selection mechanism of the polymer wrapping technique of three different polymers for semiconducting SWNTs with two different diameters. Among the three polymers, PF12 tends to be a suitable dispersant of large diameter nanotubes but not with tiny diameter nanotubes. P3DDT exhibits the best outcome regarding the selectivity towards semiconducting species, with a dispersion yield of 15% for smaller diameter nanotubes and 21% for larger diameter nanotubes.

A comprehensive experimental study was developed by Namasivayam et al., where they studied the role of polyvinylpyrrolidone molecular weight on the functionalization of various carbon nanotubes and their Composites. The results suggest that PVP improves the expression of desired properties of the CNTs as electrical, thermal, and mechanical properties as long as the length to diameter ratio of the carbon nanotube is taken into account. The higher the aspect ratio, the larger the PVP chain should be, or a low molecular weight PVP can be used in larger quantities. Similarly, for a CNT with a low aspect ratio that is found in large quantities, a PVP in a larger size or molecular weight concentration will give better results[73]. In the case of polymeric matrices, the authors mention that PVP at low concentrations about the CNT size does not contribute to improving the properties of CNTs. In contrast, an excess of PVP affects the interaction between the carbon nanotubes in the polymer matrix by disrupting the formation of a structured nanotube network through the isolation of nanotubes from their neighbors, thus compromising the effective conductive path in the overall composite.

Chapter 4

Conclusions & Outlook

In agreement with the objective one, was identified the interaction between PVP and CNT models based on the system's dynamics, quantitative information on the number of monomers interacting with the surface, the percentage of surface covered, and the distance between the CNT surface and each PVP atom. In detail, these analyses indicate that the PVP polymer shows affinity to the carbon nanotube surface by constantly interacting during the simulation. It was evidenced that the closest atoms to the CNT surface were hydrogen atoms presenting values lower than 3Å which could be sugget a non-covalent iteration. In addition, variations in the sizes of the C-C bonds were observed concerning the atoms immersed in the interaction. These observations agree with the presence of intermolecular forces acting to correspond to Van der Waals interactions. They do not chemically change the nanotube surface but are strong enough to maintain a constant interaction of the polymer and CNT.

Based on objective two, two relevant differences were to identify between the SWCNT model and the graphene layers model related to the curvature and number of layers. In first place, the curvature in the SWCNT model facilitated the linear and flexible structure of the PVP to wrapping with the CNT surface which allows to form a stable interaction that prevents the agglomeration of CNT into a matrix of composites and manipulates the CNT into ordered structure such a phenomenon does not occur with the flat graphene layered model. On the other hand, the graphene layered model evidenced larger distances between its surface and the PVP atoms than the SWCNT model. From which, it was evidenced that the amount of graphene layers influences the distances between the PVP atoms and the surface of the CNT model because the Van de Wall forces interaction between graphene layers that decreases the buckling and deformations in the top graphene sheet when a molecule is deposited.

Finally, from the graphene layer system it was concluded that the ideal amount of polymer for maximum interaction with the CNT surface is 10 polymers. It was evidenced that the 10 polymers present in the system interacted with the surface obtaining 50% of total coverage. While the system of 20 polymers presented a total coverage of 48%. This evidence shows that once the amount of 10 polymers in the system is exceeded, the surface coverage decreases although there is enough space on the surface to be occupied by the polymers present. Thus, the polymer at high concentrations prefers to interact with other PVP chains rather than with the surface of the graphene layers. On the other hand, in the SWCNT systems, partially complete coverage of the surface was obtained from all 5 polymers. As the amount of polymer in the system increased, the distance between the polymer atoms and the surface was observed to increase (see Fig. 3.5). Thus, a coverage of polymers interacting with each other was formed around the nanotube.Finally, it was concluded that the concentration of PVP does affect the interaction of PVP with the surface. When there is a lower concentration of PVP, it wraps around the nanotube surface. However, as the concentration of PVP increases, they prefer to interact with each other, creating a protective polymeric layer on the PVP (See Fig. 3.6). However, an excess of polymer on the surface would form a very thick layer of PVP and the CNT properties would be compromised, while a deficiency of polymer on the surface would not be sufficient to achieve an adequate dispersion of the nanotube in polymeric matrices.

In the next step of the project, a carbon nanotube reinforced nanocomposite system will be considered to study the effect of interaction between the polymer and CNTs on mechanical properties through molecular dynamics. The Young's modulus of the polymer and the nanotube will be evaluated separately and compared with the modulus of the system. In the same way, the tendency of tensile, strength, stiffness, and fluctuation of density will be studied. The study should consider the results of different amounts of polymers obtained in the present study to evaluate which system will provide an integral balance of the mechanical properties in the nanocomposite.

Bibliography

[1] Ibrahim, K. S. Carbon nanotubes-properties and applications: a review. *Carbon letters* **2013**, *14*, 131–144.

[2] Cha, C.; Shin, S. R.; Annabi, N.; Dokmeci, M. R.; Khademhosseini, A. Carbon-based nanomaterials: multifunctional materials for biomedical engineering. *ACS nano* **2013**, *7*, 2891–2897.

[3] Dral, P. O. *Theoretical study of electronic properties of carbon allotropes*; Friedrich-Alexander-Universitaet Erlangen-Nuernberg (Germany), 2013.

[4] O'connell, M. J. *Carbon nanotubes: properties and applications*; CRC press, 2018.

[5] Kharisov, B. I.; Kharissova, O. V. *Carbon allotropes: metal-complex chemistry, properties and applications*; Springer, 2019.

[6] Lu, W.; Baek, J.-B.; Dai, L. *Carbon nanomaterials for advanced energy systems: advances in materials synthesis and device applications*; John Wiley & Sons, 2015.

[7] Iijima, S.; Ichihashi, T. Single-shell carbon nanotubes of 1-nm diameter. *nature* **1993**, *363*, 603–605.

[8] Iijima, S. 19 9 1 Nature Publishing Group. *Nature* **1991**, *354*, 56–58.

[9] Eatemadi, A.; Daraee, H.; Karimkhanloo, H.; Kouhi, M.; Zarghami, N.; Akbarzadeh, A.; Abasi, M.; Hanifehpour, Y.; Joo, S. W. Carbon nanotubes: properties, synthesis, purification, and medical applications. *Nanoscale research letters* **2014**, *9*, 1–13.

[10] Barros, E. B.; Jorio, A.; Samsonidze, G. G.; Capaz, R. B.; Souza Filho, A. G.; Mendes Filho, J.; Dresselhaus, G.; Dresselhaus, M. S. Review on the symmetry-related properties of carbon nanotubes. *Physics reports* **2006**, *431*, 261–302.

[11] Saifuddin, N.; Raziah, A.; Junizah, A. Carbon nanotubes: a review on structure and their interaction with proteins. *Journal of Chemistry* **2013**, *2013*.

[12] Tománek, D.; Jorio, A.; Dresselhaus, M. S.; Dresselhaus, G. *Carbon Nanotubes*; Springer, 2007; pp 1–12.

[13] Huang, B. Carbon nanotubes and their polymeric composites: the applications in tissue engineering. *Biomanufacturing Reviews* **2020**, *5*, 1–26.

[14] Khan, W.; Sharma, R.; Saini, P. Carbon nanotube-based polymer composites: synthesis, properties and applications. *Carbon Nanotubes-Current Progress of their Polymer Composites* **2016**,

[15] Saliev, T. The advances in biomedical applications of carbon nanotubes. *C* **2019**, *5*, 29.

[16] Simon, J.; Flahaut, E.; Golzio, M. Overview of carbon nanotubes for biomedical applications. *Materials* **2019**, *12*, 624.

[17] Ferrier, D. C.; Honeychurch, K. C. Carbon Nanotube (CNT)-Based Biosensors. *Biosensors* **2021**, *11*, 486.

[18] Moyo, M.; Okonkwo, J. O.; Agyei, N. M. An amperometric biosensor based on horseradish peroxidase immobilized onto maize tassel-multi-walled carbon nanotubes modified glassy carbon electrode for determination of heavy metal ions in aqueous solution. *Enzyme and microbial technology* **2014**, *56*, 28–34.

[19] Peng, R.; Tang, X. S.; Li, D. Detection of Individual Molecules and Ions by Carbon Nanotube-Based Differential Resistive Pulse Sensor. *Small* **2018**, *14*, 1800013.

[20] Anshori, I.; Nuraviana Rizalputri, L.; Rona Althof, R.; Sean Surjadi, S.; Harimurti, S.; Gumilar, G.; Yuliarto, B.; Handayani, M. Functionalized multi-walled carbon nanotube/silver nanoparticle (f-MWCNT/AgNP) nanocomposites as non-enzymatic electrochemical biosensors for dopamine detection. *Nanocomposites* **2021**, *7*, 97–108.

[21] Holban, A. M.; Grumezescu, A. M. *Nanoarchitectonics for Smart Delivery and Drug Targeting*; William Andrew, 2016.

[22] Maiti, D.; Tong, X.; Mou, X.; Yang, K. Carbon-based nanomaterials for biomedical applications: a recent study. *Frontiers in pharmacology* **2019**, 1401.

[23] others,, *et al.* Carbon nanotube multilayered nanocomposites as multifunctional substrates for actuating neuronal differentiation and functions of neural stem cells. *Biomaterials* **2018**, *175*, 93–109.

[24] Kharaziha, M.; Shin, S. R.; Nikkhah, M.; Topkaya, S. N.; Masoumi, N.; Annabi, N.; Dokmeci, M. R.; Khademhosseini, A. Tough and flexible CNT–polymeric hybrid scaffolds for engineering cardiac constructs. *Biomaterials* **2014**, *35*, 7346–7354.

[25] Flores-Cedillo, M.; Alvarado-Estrada, K.; Pozos-Guillén, A.; Murguía-Ibarra, J.; Vidal, M.; Cervantes-Uc, J.; Rosales-Ibáñez, R.; Cauich-Rodríguez, J. Multiwall carbon nanotubes/polycaprolactone scaffolds seeded with human dental pulp stem cells for bone tissue regeneration. *Journal of Materials Science: Materials in Medicine* **2016**, *27*, 1–12.

[26] The role of the iron catalyst in the toxicity of multi-walled carbon nanotubes (MWCNTs). **2017**, *43*.

[27] Pulskamp, K.; Diabaté, S.; Krug, H. F. Carbon nanotubes show no sign of acute toxicity but induce intracellular reactive oxygen species in dependence on contaminants. *Toxicology letters* **2007**, *168*, 58–74.

[28] Jiang, W.; Wang, Q.; Qu, X.; Wang, L.; Wei, X.; Zhu, D.; Yang, K. Effects of charge and surface defects of multi-walled carbon nanotubes on the disruption of model cell membranes. *Science of the Total Environment* **2017**, *574*, 771–780.

[29] Lanone, S.; Andujar, P.; Kermanizadeh, A.; Boczkowski, J. Determinants of carbon nanotube toxicity. *Advanced drug delivery reviews* **2013**, *65*, 2063–2069.

[30] Fujigaya, T.; Nakashima, N. Non-covalent polymer wrapping of carbon nanotubes and the role of wrapped polymers as functional dispersants. *Science and technology of advanced materials* **2015**,

[31] Norizan, M. N.; Moklis, M. H.; Demon, S. Z. N.; Halim, N. A.; Samsuri, A.; Mohamad, I. S.; Knight, V. F.; Abdullah, N. Carbon nanotubes: Functionalisation and their application in chemical sensors. *RSC advances* **2020**, *10*, 43704–43732.

[32] Fatemi, S. M.; Foroutan, M. Recent developments concerning the dispersion of carbon nanotubes in surfactant/polymer systems by MD simulation. *Journal of Nanostructure in Chemistry* **2016**, *6*, 29–40.

[33] Ma, P.-C.; Siddiqui, N. A.; Marom, G.; Kim, J.-K. Dispersion and functionalization of carbon nanotubes for polymer-based nanocomposites: A review. *Composites Part A: Applied Science and Manufacturing* **2010**, *41*, 1345–1367.

[34] Koczkur, K. M.; Mourdikoudis, S.; Polavarapu, L.; Skrabalak, S. E. Polyvinylpyrrolidone (PVP) in nanoparticle synthesis. *Dalton Transactions* **2015**, *44*, 17883–17905.

[35] Jadhav, S.; Nikam, D.; Khot, V.; Thorat, N.; Phadatare, M. R.; Ningthoujam, R.; Salunkhe, A.; Pawar, S. Studies on colloidal stability of PVP-coated LSMO nanoparticles for magnetic fluid hyperthermia. *New Journal of Chemistry* **2013**, *37*, 3121–3130.

[36] Kurakula, M.; Rao, G. K. Moving polyvinyl pyrrolidone electrospun nanofibers and bioprinted scaffolds toward multidisciplinary biomedical applications. *European Polymer Journal* **2020**, *136*, 109919.

[37] Awasthi, R.; Manchanda, S.; Das, P.; Velu, V.; Malipeddi, H.; Pabreja, K.; Pinto, T. D.; Gupta, G.; Dua, K. *Engineering of Biomaterials for Drug Delivery Systems*; Elsevier, 2018; pp 255–272.

[38] Robinson, B. V.; Sullivan, F.; Borzelleca, J. F.; Schwartz, S. *PVP: a critical review of the kinetics and toxicology of polyvinylpyrrolidone (povidone)*; CRC Press, 2018.

[39] Kurakula, M.; Rao, G. K. Pharmaceutical assessment of polyvinylpyrrolidone (PVP): As excipient from conventional to controlled delivery systems with a spotlight on COVID-19 inhibition. *Journal of Drug Delivery Science and Technology* **2020**, *60*, 102046.

[40] Nair, B. Final report on the safety assessment of polyvinylpyrrolidone (PVP). *International journal of toxicology* **1998**, *17*, 95–130.

[41] Kimaro, E.; Tibalinda, P.; Shedafa, R.; Temu, M.; Kaale, E. Formulation development of chewable albendazole tablets with improved dissolution rate. *Heliyon* **2019**, *5*, e02911.

[42] Franco, P.; De Marco, I. The Use of Poly (N-vinyl pyrrolidone) in the Delivery of Drugs: A Review. *Polymers* **2020**, *12*, 1114.

[43] Miller, L.; Hamm, F. Macromolecular properties of polyvinylpyrrolidone: molecular weight distribution. *The Journal of Physical Chemistry* **1953**, *57*, 110–122.

[44] Teodorescu, M.; Bercea, M. Poly (vinylpyrrolidone)–a versatile polymer for biomedical and beyond medical applications. *Polymer-Plastics Technology and Engineering* **2015**, *54*, 923–943.

[45] INCHEM, 493. Polyvinylpyrrolidone (PVP) (WHO Food Additives Series 15). `https://inchem.org/documents/jecfa/jecmono/v15je08.htm`.

[46] ASHLAND, With good chemistry great things happen. ™. *c*

[47] Sun, J.; Yu, X.; Zhang, Q.; Ling, Y.; Yang, Z. Stable CO anti-poisoning and high durability of a Pt electrocatalyst supported on carbon nanotubes. *RSC advances* **2017**, *7*, 39767–39772.

[48] Haghighat, F.; Mokhtary, M. Preparation and characterization of polyvinylpyrrolidone/magnetite decorated carboxylic acid functionalized multi-walled carbon nanotube (PVP/MWCNT-Fe3O4) nanocomposite. *Journal of Inorganic and Organometallic Polymers and Materials* **2017**, *27*, 779–787.

[49] Bulbul, Y. E.; Eskitoros-Togay, Ş. M.; Demirtas-Korkmaz, F.; Dilsiz, N. Multi-walled carbon nanotube-incorporating electrospun composite fibrous mats for controlled drug release profile. *International Journal of Pharmaceutics* **2019**, *568*, 118513.

[50] Maziukiewicz, D.; Maciejewska, B. M.; Litowczenko, J.; Kościński, M.; Warowicka, A.; Wychowaniec, J. K.; Jurga, S. Designing biocompatible spin-coated multiwall carbon nanotubes-polymer composite coatings. *Surface and Coatings Technology* **2020**, *385*, 125199.

[51] Tserpes, K. I.; Silvestre, N. *Modeling of carbon nanotubes, graphene and their composites*; Springer, 2014; Vol. 188.

[52] Meng, J. *A study of the polymer-cnt interactions in polymer/cnt composites using experimental and computational methods*; Northeastern University, 2015.

[53] Case, D. A.; Cheatham III, T. E.; Darden, T.; Gohlke, H.; Luo, R.; Merz Jr, K. M.; Onufriev, A.; Simmerling, C.; Wang, B.; Woods, R. J. The Amber biomolecular simulation programs. *Journal of computational chemistry* **2005**, *26*, 1668–1688.

[54] Allouche, A.-R. Gabedit—A graphical user interface for computational chemistry softwares. *Journal of computational chemistry* **2011**, *32*, 174–182.

[55] van Gunsteren, W. F.; Billeter, S.; Eising, A.; Hünenberger, P.; Krüger, P.; Mark, A.; Scott, W.; Tironi, I. Biomolecular simulation: the GROMOS96 manual and user guide. *Vdf Hochschulverlag AG an der ETH Zürich, Zürich* **1996**, *86*, 1–1044.

[56] others,, *et al.* The GROMOS software for biomolecular simulation: GROMOS05. *Journal of computational chemistry* **2005**, *26*, 1719–1751.

[57] Durrant, J. D.; McCammon, J. A. Molecular dynamics simulations and drug discovery. *BMC biology* **2011**, *9*, 1–9.

[58] Cheng, X.; Ivanov, I. Molecular dynamics. *Computational toxicology* **2012**, 243–285.

[59] Ayappa, K. Lecture Notes: Molecular Dynamics Simulations.

[60] Gullingsrud, J.; Saam, J.; Phillips, J. psfgen User's Guide. *Urbana* **2006**, *51*, 61801.

[61] Humphrey, W.; Dalke, A.; Schulten, K. VMD: visual molecular dynamics. *Journal of molecular graphics* **1996**, *14*, 33–38.

[62] Humphrey, D. A., W.; Schulten, K. *VMD - Visual Molecular Dynamics*; J. Molec. Graphics, 1996; Vol. 14.1.

[63] JDC, P. J. H. D. M.; RC, S. J. R. J. B. Buch R. *Fiorin G. Hénin J. Jiang W. McGreevy R. Melo MCR Radak B. Skeel RD Singharoy A. et al., Scalable molecular dynamics on CPU and GPU architectures with NAMD. J. Chem. Phys* **2020**, *153*, 044130.

[64] Feller, S. E.; Zhang, Y.; Pastor, R. W.; Brooks, B. R. Constant pressure molecular dynamics simulation: The Langevin piston method. *The Journal of chemical physics* **1995**, *103*, 4613–4621.

[65] Hopkins, C. W.; Le Grand, S.; Walker, R. C.; Roitberg, A. E. Long-time-step molecular dynamics through hydrogen mass repartitioning. *Journal of chemical theory and computation* **2015**, *11*, 1864–1874.

[66] Chik, M. W.; Hussain, Z.; Zulkefeli, M.; Tripathy, M.; Kumar, S.; Majeed, A. B. A.; Byrappa, K. Polymer-wrapped single-walled carbon nanotubes: A transformation toward better applications in healthcare. *Drug delivery and translational research* **2019**, *9*, 578–594.

[67] O'Connell, M. J.; Boul, P.; Ericson, L. M.; Huffman, C.; Wang, Y.; Haroz, E.; Kuper, C.; Tour, J.; Ausman, K. D.; Smalley, R. E. Reversible water-solubilization of single-walled carbon nanotubes by polymer wrapping. *Chemical physics letters* **2001**, *342*, 265–271.

[68] Zheng, Q.; Xue, Q.; Yan, K.; Hao, L.; Li, Q.; Gao, X. Investigation of molecular interactions between SWNT and polyethylene/polypropylene/polystyrene/polyaniline molecules. *The Journal of Physical Chemistry C* **2007**, *111*, 4628–4635.

[69] Huang, Y.; Zheng, Y.; Song, W.; Ma, Y.; Wu, J.; Fan, L. Poly (vinyl pyrrolidone) wrapped multi-walled carbon nanotube/poly (vinyl alcohol) composite hydrogels. *Composites Part A: Applied Science and Manufacturing* **2011**, *42*, 1398–1405.

[70] Georgakilas, V.; Tiwari, J. N.; Kemp, K. C.; Perman, J. A.; Bourlinos, A. B.; Kim, K. S.; Zboril, R. Noncovalent functionalization of graphene and graphene oxide for energy materials, biosensing, catalytic, and biomedical applications. *Chemical reviews* **2016**, *116*, 5464–5519.

[71] Manivannan, S.; Jeong, I. O.; Ryu, J. H.; Lee, C. S.; Kim, K. S.; Jang, J.; Park, K. C. Dispersion of single-walled carbon nanotubes in aqueous and organic solvents through a polymer wrapping functionalization. *Journal of Materials Science: Materials in Electronics* **2009**, *20*, 223–229.

[72] others,, *et al.* Van der Waals force: a dominant factor for reactivity of graphene. *Nano letters* **2015**, *15*, 319–325.

[73] Namasivayam, M.; Andersson, M. R.; Shapter, J. G. A Comparative Study on the Role of Polyvinylpyrrolidone Molecular Weight on the Functionalization of Various Carbon Nanotubes and Their Composites. *Polymers* **2021**, *13*, 2447.